UNIVERSITI TEKNIKAL MALAYSIA MELAKA

FACULTY OF ELECTRICAL ENGINEERING

FINAL YEAR PROJECT REPORT

Name	**:**	**Carolyn Lim Kim Yen**
Course	**:**	**4BEKP S2**
Matric Number	**:**	**B011010361**
Project Title	**:**	**Performance Analysis of Power Quality Monitoring System**
Supervisor	**:**	**Nur Hazahsha binti Shamsudin**

PERFORMANCE ANALYSIS OF POWER QUALITY MONITORING SYSTEM

Carolyn Lim Kim Yen

Bachelor of Electrical Engineering (Industrial Power)

June 2014

"I hereby declare that I have read through this report entitled "Performance Analysis of Power Quality Monitoring System" and found that it has comply the partial fulfilment for awarding the degree of *Bachelor of Electrical Engineering (Industrial Power)*"

Signature : .....

Supervisor's Name : .....

Date : .....

PERFORMANCE ANALYSIS OF POWER QUALITY MONITORING SYSTEM

CAROLYN LIM KIM YEN

This report is submitted in partial fulfilment of requirement for the degree of Bachelor in Electrical Engineering (Industrial Power)

Faculty of Electrical Engineering

UNIVERSITI TEKNIKAL MALAYSIA MELAKA

2014

I declare that this report entitled “Performance Analysis of Power Quality Monitoring System” is the result of my own research except as cited in the references. The report has not been accepted for any degree and is not concurrently submitted in candidature of any other degree.

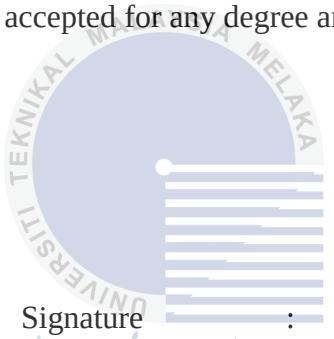

Signature : .....

Name : .....

Date : .....

ACKNOWLEDGEMENT

I would like to express my earnest gratitude to each and every one who had helped me, either directly or indirectly, to carry out the research.

First of all, I would like to express my appreciation and deep respect to my supervisor, Cik Nur Hazahsha binti Shamsudin for the supervision and guidance given throughout the Final Year Project 2. Her knowledge, advice and encouragement have helped me to overcome the problems faced in the project.

My thanks and appreciation also goes to my parents and family for their understanding, cooperation, suggestions, and support during the whole process of conducting research for the project.

Last but not the least, thanks is given to all of my friends and everyone who has contributed in helping me to complete the Final Year Project 2.

ABSTRACT

The presence of power quality (PQ) problem in the power supply system can cause malfunction of the modern high technology devices and these faults will bring about immense financial losses in the commercial and industrial sectors. Essentially, there is a need to determine the type of PQ problem that occurred, so that proper actions can be taken to overcome the problem. Most of the PQ instruments available in the market are unable to classify PQ events, thus power quality monitoring system (PQMS) is developed by previous researchers to solve that problem. The flexibility of PQMS has facilitated in identifying PQ problem that is globally experienced in real electrical delivery of power system prominently in distribution. It is suitable for remote measurement of various non-linear loads, as well as instantaneous classification of the PQ problem. The validation of PQMS performance in measurements and PQ detection through numerous laboratory experiments is feasible by using Fluke 43B power quality analyser (PQA) as the reference tool. Five different set-ups with components like three phase induction motor, single phase capacitor run motor and single phase full wave controlled rectifier are constructed for no load test, blocked rotor test, voltage sag and harmonic distortion in single phase and three phase system. The no load and blocked rotor tests data collection inclusive of voltage, current, real power, reactive power, apparent power and power factor has prompted the measurement accuracy assessments. The voltage sag and harmonic distortion are induced for testing the PQMS ability in identifying the signal disturbances. The effectiveness of PQMS is emphasized through the comparisons between the signals obtained and absolute percent error (APE) of the measurements with the results of PQA. In short, the performance of PQMS in signal detection and measurement is verified.

ABSTRAK

Kewujudan masalah kualiti kuasa (PQ) dalam sistem bekalan kuasa boleh menyebabkan kerosakan peranti-peranti modern yang berteknologi tinggi dan kerosakan tersebut akan membawa kerugian yang banyak dalam sektor perdagangan dan perindustrian. Ia adalah penting untuk menentukan jenis masalah PQ supaya tindakan yang sesuai boleh diambil untuk menyelesaikan masalah tersebut. Kebanyakan peralatan PQ yang ada dalam pasaran tidak mampu untuk mengklasifikasikan masalah PQ, oleh itu sistem pemantauan kualiti kuasa (PQMS) telah dicadangkan oleh penyelidik sebelum ini untuk mengatasi kelemahan tersebut. Fleksibiliti PQMS telah memudahkan identifikasi masalah PQ yang dialami secara global dalam penghantaran bekalan kuasa menerusi sistem pengedaran. Ia juga sesuai bagi ukuran jauh untuk pelbagai jenis beban tidak linear serta klasifikasi masalah PQ dengan kadar segera. Pengesahan pretasi PQMS dalam ukuran dan pengesanan masalah PQ melalui pelbagai eksperimen makmal boleh dilaksanakan dengan menggunakan penganalisis kualiti kuasa (PQA) Fluke 43B sebagai rujukan. Lima eksperimen dengan komponen yang berbeza seperti motor tiga fasa, motor kapasitor larian fasa tunggal, dan rektifier gelombang penuh terkawal telah digunakan untuk ujian tanpa beban, ujian pemutar tersekat, pengenduran voltan dan herotan harmonik dalam sistem fasa tunggal dan tiga fasa. Data-data seperti voltan, arus, kuasa sebenar, kuasa reaktif, kuasa ketara dan faktor kuasa yang dikumpul melalui ujian tanpa beban dan ujian pemutar tersekat telah mendorong penilaian ketepatan pengukuran. Di samping itu, pengenduran voltan dan herotan harmonik dalam sistem fasa tunggal dan tiga fasa adalah bertujuan untuk menguji keupayaan PQMS dalam mengenal pasti gangguan isyarat. Keberkesanan PQMS telah ditekankan melalui perbandingan antara isyarat diperolehi dan peratusan ralat mutlak (APE) dalam ukuran dengan keputusan yang diperoleh PQA. Kesimpulannya, prestasi PQMS dalam pengesanan isyarat dan pengukuran telah disahkan.

TABLE OF CONTENTS

LIST OF TABLES

LIST OF FIGURES

LIST OF ABBREVIATIONS

AC	-	Alternating current
ADALINE	-	Adaptive Linear Neural Network
ADC	-	Analogue to digital
APE	-	Absolute percent error
ASD	-	Adjustable speed drives
AWG	-	Arbitrary waveform generator
DAQ	-	Data acquisition
DC	-	Direct current
EAF	-	Electric arc furnace
EMI	-	Electromagnetic interference
FFT	-	Fast Fourier transform
FKE	-	Faculty of Electrical Engineering
GUI	-	Graphical user interface
HOS	-	Higher-order statistics
I/O	-	Input/output
IEC	-	International Electrotechnical Commission
IEEE	-	Institute of Electrical and Electronics Engineers
IGBT	-	Insulated gate bipolar transistor

IPC	-	Industrial Power Corruptor
NI	-	National Instrument
PC	-	Personal computer
PLL	-	Phase-locked-loop
PQ	-	Power quality
PQA	-	Power quality analyser
PQMS	-	Power quality monitoring system
RLC	-	Resistive, inductive and capacitive
rms	-	Root mean square
SCR	-	Silicon controlled rectifier
SRPA	-	Smart recording power analyser
STFT	-	Short time Fourier transform
TFR	-	Time frequency representation
THD	-	Total harmonic distortion
UPS	-	Uninterruptable power supply
USB	-	Universal Serial Bus
VI	-	Virtual instrument

LIST OF APPENDICES

CHAPTER 1

INTRODUCTION

1.1 Research Background

Power quality (PQ) is a set of parameters that delineate the properties of power supplied to the users in terms of supply continuity and voltage characteristics during typical operating conditions [1]. The deviations of voltage, current or frequency from its constant magnitude and ideal sinusoidal waveform can induce failure in any sensitive electric equipment. There are six categories of common PQ problems, namely voltage fluctuation, harmonic distortion, power frequency variation, undervoltage or overvoltage, voltage sag or swell, and transients. These issues have always been present in the power supply system, but they are not in the limelight until recently due to the intensified usage of power electronic gadgets. Non-linear loads which have become a prominent part in the industrial and commercial power systems tempt to draw non-sinusoidal currents from the supply, thus inducing voltage distortion and affecting the power factor [2]. Since the control system equipped in the devices can be malfunctioned due to the varying supply conditions, this justify that the modern electronic devices in electrical system are more sensitive to PQ issues than those from the olden days. For instance, the proper operation of high technology electricity dependent devices and instruments depends on the voltage quality supplied to them.

This project intends to analyse the performance of Power Quality Monitoring System (PQMS) and determine its functionality in the practical environment. Besides measuring voltage, current, real power, reactive power, apparent power and power factor,

PQMS [3] is also capable in classifying the PQ problem being measured. Hence, users can identify the PQ problem instantly without struggling to pinpoint the problem from the recorded signal. For example, if sag occurred in the system during the monitoring, the word "sag" will be displayed in the graphical user interface. Another feature of this PQMS is data recording. As the name "Real Time Power Quality Monitoring System" implies, it can monitor the power system in real time, where the changes occurred in the power system can be recorded and saved as a text file in the PQMS for further analysis. The PQMS is proposed to serve as an alternative to the pricy PQ measuring instruments available in the market, so it is necessary to compare the performance and capability of the PQMS with those equipment accordingly.

Theoretically, PQMS is capable of measuring and detecting the PQ problems. Hence, laboratory testing is carried out for the system performance verification. There are two methods for producing PQ problem signals, i.e. signal generator and experimental set up [4]. Although an ideal signal waveform can be generated from signal generator, it does not mean that particular signal will also occurred in the real world. However, it is a good choice if one does not have access to the vast choices of equipment to set up an experiment. The downside of using experimental set up is the condition of the equipment. For instance, after running for a long time, a motor will be heated and thus affecting the output. The efficiency of a piece of worn out equipment is also low compared to the new ones. Despite the drawbacks disclosed earlier, the output from an experimental set up represents best on the phenomena that could happen in a real world situation.

1.2 Problem Statement

PQMS has been tested through simulation by the previous researchers [3]. The simulation results showed that the system can measure and classify PQ problems. Although the system has passed the simulation testing, but it does not prove that it will be able to give similar performance in the real world situation measurements and classification. The performance of the developed monitoring system needs to be

determined so that PQMS can serve as one of the alternative instruments used for PQ monitoring in practical environment.

1.3 Objectives

This project primarily focused on achieving the following objectives:

i) To test PQMS aptitude in power system measurements through voltage-varying experimental set ups.

ii) To generate voltage sag and harmonic signals through laboratory experiments for verifying PQMS ability in classifying PQ problem.

iii) To analyse the performance of the PQMS in reference with Fluke 43B PQA.

1.4 Scope

In order to validate the performance of PQMS in terms of measurements and PQ disturbances classification, various experiments are conducted in the laboratories at Faculty of Electrical Engineering (FKE), UTeM and all the experimental outcomes are compared with the data logged by Fluke 43B PQA. Three phase squirrel cage induction motor no load test and blocked rotor test are chosen for testing the PQMS accuracy in measuring six types of power system parameters which include voltage, current, real power, reactive power, apparent power and power factors. There are two types of PQ problem in single phase and three phase systems concerned in this project, for instance voltage sag and harmonic distortion.

1.5 Project Outcome

Five different laboratory experiments are conducted to determine the accuracy of PQMS in taking measurements as well as the efficiency in identifying the PQ problems. Fluke 43B PQA is chosen as the reference instrument because it can perform all the measurements that are required in this project. Through the no load test and blocked rotor test, the PQMS accuracy in measuring the distinctive power system parameters such as voltage, current, real power, reactive power, apparent power and power factor has been ascertained with the APE calculated from the results obtained by PQA and PQMS. The mean APE from each parameter further justified the performance of PQMS.

Voltage sag signals in single phase system are generated with two different loads, for instance six capacitor run motors and four capacitor run motors with RLC load. These two types of load managed to cause a voltage drop which is more than 10% of the nominal 240V, thus satisfying the IEEE definition for sag. When the three phase motor is started up, the phase to phase measurement at the supply also presented similar trend. During the drop in voltage due to motor starting, PQMS has successfully classified the voltage drop as "sag". Fluke 43B PQA does not have the function to categorize the voltage drop as "sag", but through calculation and analysis, the signals have confirmed to demonstrate voltage sag during the motor starting.

Other than voltage sag, harmonic distortion is another PQ event concerned. The harmonic voltage and current signals from the single phase full wave controlled rectifier and three phase induction motor are logged with PQA and PQMS. The representation of total harmonic distortion (THD) is different for the two instruments. Although THD is displayed as number and line graph in PQA and PQMS respectively, but the value shown by the instruments are similar. Only the signal distortion in full wave controlled rectifier is categorized as "Harmonic". Although there are certain percentage of THD present in the three phase induction motor signals, but they are not considered by PQMS as harmonics.

1.6 Thesis Outline

Chapter 2 presents the background theories related to the project. The theories covered are PQ, transients, waveform distortion, voltage sag and voltage swell. The summary and discussion of the previous related works by many researchers has also included in this chapter.

Chapter 3 gives details on the methodology used in the project. The reference instrument, components in PQMS as well as experiment procedure flowcharts are briefly described prior to the detailed description of three categories of experimental set ups used for the performance validation.

Chapter 4 analyses the outcomes from the experiments considered in chapter 3. These results are organized into different sections and they are represented in the form of tables, graphs and diagrams necessarily. The effectiveness of PQMS in measurements and PQ disturbance classifications are discussed in accordance with the results recorded by PQA. Additionally, the inclusion of comparison between the cases shows the effect of different load setting in the experimental outcomes.

Chapter 5 concludes the study of performance of PQMS proposed and summarizes the findings from the experiments. Some future work recommendations are also suggested for improving the methods used in determining the performance of PQMS.

CHAPTER 2

LITERATURE REVIEW

2.1 Introduction

Comprehension of a topic greatly affects the research progress because without proper knowledge, the researchers will not be able to recommend the probable method that is suitable for their researches, as well as elucidations for the problems arise during research. This chapter outlines the related theory and principles, review and discussion on the journals. The term "power quality" is first defined with the definition from Institute of Electrical and Electronics Engineers (IEEE), followed with discussion on the rising interest in PQ and problems that it introduced to the power system and also the end users. The PQ phenomena which occurred in the power system can be sorted into two categories, namely steady-state variations and disturbances. Transients, waveform distortion, voltage sag and voltage swell are briefly discussed in terms of their definitions, causes and impacts.

The review of various previous related works focused on the techniques to test the PQ detection instrument designed by respective researchers. Simulations, laboratory experiments and on-site testing are the three types of testing performed by these researchers. The instruments generally made up of three sections, i.e. input, interfacing device, and displaying unit. The existence of numerous algorithms had encouraged the development and improvement of PQ monitoring instruments. A reference unit is required for performance analysis of the system whereby comparisons of their results can determine the effectiveness of the system proposed in measurements and PQ identifications.

2.2 Theory and Basic Principles

According to IEEE [5], PQ is "the concept of powering and grounding electronic equipment in a manner that is suitable to the operation of that equipment and compatible with the premise wiring system and other connected equipment." PQ can be seen as the compatibility between the quality of voltage supplied and the proper operation of equipment [6]. It is also related with economics, in terms of obtaining the optimum level of investment for power system and equipment. This is to achieve compatibility with minimum cost.

There are several reasons stated in [7] for the increasing interest in PQ. One of them is malfunction of equipment caused by their intolerance towards voltage quality disturbances. The incorrect operation resulted in production stoppage which leads to losses in profit and higher cost of maintenance. Voltage sags along with long and short interruptions are identified as the main culprits that contributed to this problem. Besides that, a great number of power equipment has been powered by power electronic devices. The broad spectrum of current distortion produced by these devices has influenced the occurrence of harmonic distortion in the power supply system.

PQ is becoming a greater concern now. The increasing number of power electronics equipment affects the quality of electric power supply. This is because harmonics are produced by the industrial loads and domestics loads into the network. Ironically, these disturbance-causing equipment are sensitive to the deviations in supply. For example, the transient power fluctuation can interrupt the high-speed processes in factories, and momentary power sag can affect the fault-intolerant information technologies in the commercial firms [8]. As a result, industrial and commercial customers suffered financial losses. PQ problem in distribution system can cause the power supplied to the customers being less than the optimum value. Although residential customers do not suffer direct financial losses from the PQ problem, their satisfaction towards utility supplier will decrease [9]. This will cause the utility company to lose their customers.

PQ variations can be divided into two categories, which are steady-state variations and disturbances [10]. Voltage sag, voltage swell and transients are the example for disturbance. Disturbances are measured when an abnormality in the voltage or current is triggered. On the other hand, harmonic distortion and flicker are categorized as steady-state

variation where the measurement for this variation is done by sampling the voltage and/or current over time. There are various types of PQ problems, but voltage sag and harmonic distortion are selected in this project for the purpose of verifying the performance of PQMS.

2.2.1 Transients

The distortion produced from unwanted, fast-duration and short duration events are known as transients. Transients can be categorized as impulsive transient and oscillatory transient [11]. Figure 2.1 and Figure 2.2 below show the impulsive transient and oscillatory transient [12]. Impulsive transient is a sudden unidirectional frequency change in steady-state voltage and/or current. It also has fast rise and decay times. Lightning is the most common cause of impulsive transient. Unlike impulsive transient, oscillatory transients are sudden bidirectional frequency change in steady-state voltage and/or current. Capacitor bank switching and fast-acting over-current protective devices are some of the reasons which caused oscillatory transient to happen. Failure of a transformer, capacitor or semiconductor due to transients can bring towards faulty operation.

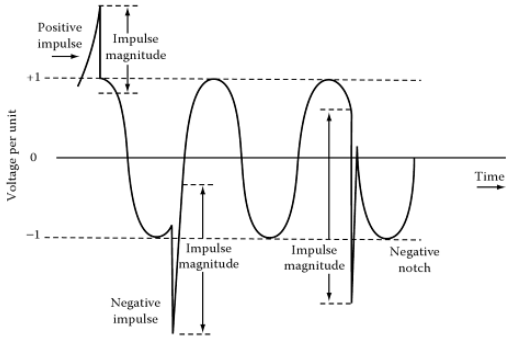

Figure 2.1: Impulsive Transient

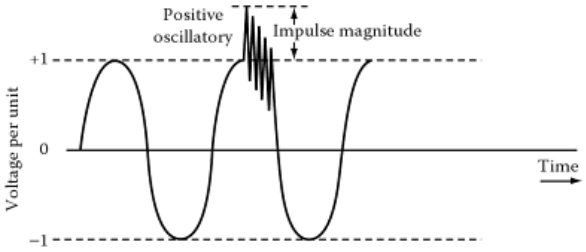

Figure 2.2: Oscillatory Transient

2.2.2 Voltage Sag and Voltage Swell

According to IEEE [5], voltage sag is a short term, few cycles duration voltage drop between 0.1 and 0.9 pu; whereas voltage swell is a short term, few cycles duration increase in voltage between 1.1 and 1.8 pu. The waveforms for voltage sag and voltage swell are depicted in Figure 2.3 and Figure 2.4 respectively [11]. Voltage sag can be caused by voltage drop from starting big motors across the line, or from a fault on the adjacent power line. The causes of voltage swell are shedding of a large load, energizing of a capacitor bank, and single line-to-ground fault. When sag occurred, the equipment tolerance towards low voltage will determine the severity of damage imposed on the equipment. Electronic drives and converters are some of the examples of equipment that are sensitive to sag. Light bulbs may burn out during swell and thus lead to safety problems.

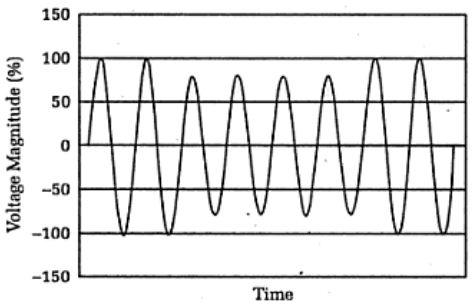

Figure 2.3: Voltage Sag

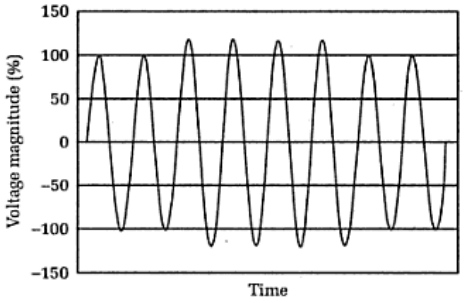

Figure 2.4: Voltage Swell

2.2.3 Waveform Distortion

The degree to which the waveform distorts from a sine wave is known as waveform distortion. IEEE has categorized direct current (DC) offset, harmonics, inter-harmonics, notching and electric noise as the five primary types of waveform distortion [5].

DC offset is defined as the presence of a DC current and/or voltage component in an alternating current (AC) system [5]. The geomagnetic disturbance and half-wave rectification are two of the reasons DC offset happens.

Inter-harmonics are frequency components of distorted voltages that are not multiples of the fundamental frequency, which resulted from cycloconverter, arc furnaces, and adjustable speed drives (ASDs) with insufficient dc link filtering [13]. Inter-harmonics can leads to excitation of low frequency mechanical oscillations, and malfunction in ripple control. Harmonics, which can be caused by rectifiers and inverters, are the inverse of inter-harmonics where they are frequency components of distorted voltages that are multiples of the fundamental frequency. Figure 2.5 presents the harmonic waveform [11]. Some of the harmonic effects are decreased in overall energy efficiency, overheating and losses in neutral line due to triplen harmonics, and increased possibility of resonance.

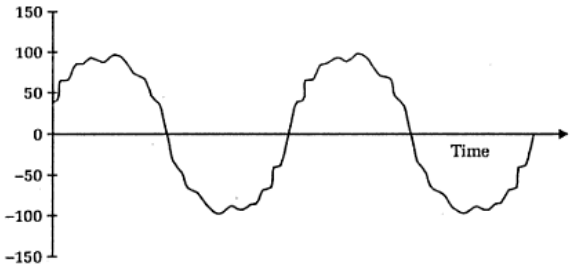

Figure 2.5: Harmonic Distortion

Notching, as shown in Figure 2.6, is resulted from a converter operation [5]. The periodic voltage disturbances do not usually cause problems because they are controlled by circuit elements related to switching devices [13] but they can be a problem in weak electric systems. Noise current produced can results in control system mis-operation whereas notching can cause faulty silicon controlled rectifier (SCR) triggering.

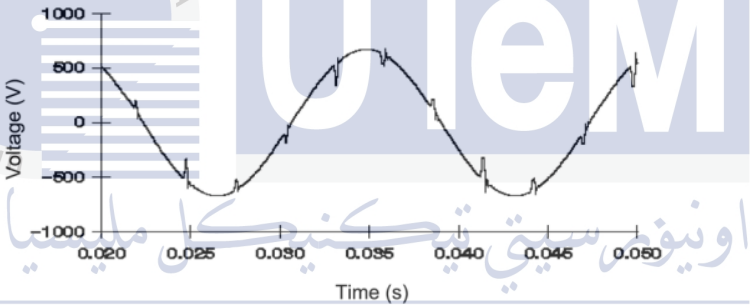

Figure 2.6: Notching

IEEE defined noise as “the unwanted electrical signals with broadband spectral content typically lower than 200 kHz, superimposed upon the power system voltage or current in the phase conductors or unwanted electrical signals found on neutral conductors or signal lines. [5]” Insulated gate bipolar transistor (IGBT) inverters’ fast switching speed and high input impedance make it possible to create stray currents resulting in electromagnetic interference (EMI). Stray current can interfere with the operation of communication equipment, adjustable speed drive (ASD) control, and barcode scanners [13].

2.3 Review of Previous Related Work

The requirement of identifying and categorizing the PQ signals for analysis has stimulated the development of PQ signals classification system [3]. The proposals of various time-frequency techniques like wavelet transform, short time Fourier transform (STFT), Gabor transform, S-transform, and spectrogram have overcome the Fourier transform limitation in tracking the variations in magnitude, frequency, or phase effectively. Therefore, spectrogram is instigated in this system whereby the signals are characterized in time frequency representation (TFR). The rule based classifier, with its setting referred to IEEE 1159-2009 standard, categorizes the signals based on signal characteristics. The sequences in the rule based classifier are swell, sag, interruption, transient, harmonic, inter-harmonic, and normal. When the signal does not meet the threshold requirement for swell, it will be analysed with the sag setting in the next stage. If the signal failed to meet the sag requirement, the continuous designation will last until it is classified as normal in the last stage. The system proposed consists of voltage and current transducers as the measuring tools to step down and isolate the inputs, DAQ card as the interfacing system between input and output, and computer as the output tool to display the results.

The computer based DAQ system in [4] comprising of LabVIEW-developed virtual instrument (VI) and NI 6034-E DAQ card offered real time monitoring of voltage and current with remote monitoring feature. A special feature of this system is it can trigger an automated email notification during the detection of disturbance and fault occurrence. Data acquisition and data analysis programs are the two main programs that made up the system. Six channels are used in this system for three phase voltage and current measurements. Several experiments are conducted to test the DAQ system. In one of the experiments, the disturbance magnitude and duration of voltage sags and swells generated with Industrial Power Corruptor (IPC) are recorded by the DAQ system. The system accuracy is then determined through the data comparison between DAQ system and IPC. Two cases of full load motor starting, i.e. one is started in normal condition while the other one is during voltage sag, are used for obtaining the voltage sag signals. Short circuit faults on the motor during full load, half load and no load are also created to test the DAQ system. Double line to ground fault and double line fault on phase one and phase two are taken into

consideration for this experiment. The DAQ system is also assigned to monitor the voltage supply in a lab for seven days continuously.

In [14], IEC 61000-4-30, the international standard that indicates how PQ should be measured, is the primary reference used for the PQ monitoring instruments. Only some of the PQ problems are being considered. Examples are supply voltage dips and interruption, voltage and current harmonics and inter-harmonics, and also voltage fluctuation. In order to carry out the test, a hardware test system is constructed. The software, that is used to implement the test procedures and coordinate the devices, is developed in LabVIEW. The PQ meters used for testing are the commercial instrument Fluke 1745 series three-phase PQ loggers memobox and a prototype implementation of a PQ meter based on DAQ board and proper software developed at the EMC-Lab of the Second University of Naples (UNI-Proto). A certain PQ phenomenon with known level is supplied to the instruments. The comparisons between the supplied value and measured value give rise to the calculation of measurement error and analysis on the instrument's performance.

The development of virtual multifunction PQA [15] is based on the adaptive linear neural network (ADALINE). It is noticed that different algorithms are used for each type of PQ problem. For instance, synchronization of PQ equipment is performed through phase-locked-loop-based technique for stationary and transient disturbances. Besides, synchronized root mean square (rms) calculation is applied in voltage dip measurement. Other than that, developed frequency estimation method and finite-impulse-response filter are integrated in a digital harmonic analyser. These findings show that it is crucial to incorporate different types of PQ disturbances algorithms in order to establish a digital multifunction analyser. This multifunction PQA, developed in LabVIEW, is a device that combines analogue-to-digital conversion (ADC) and related signal conditioning modules with the personal computer (PC). Assessment is carried out with the aid of DAQ card and signals obtained from the arbitrary waveform generator (AWG) with input/output (I/O) connector. The waveform of the measured signal is observed through a digital phosphor oscilloscope. Six cases of testing are performed, namely testing for estimation of power system frequency deviation and harmonics/inter-harmonics, testing for assessment of flickers, testing for detection and classification of voltage events, actual measurements from UPS, actual measurements from ac electric arc furnace (EAF), and actual measurements from a substation. The accuracy and efficiency of the multifunction PQA is verified by comparing the estimation results to the reference signal generated by AWG.

PQ data logger PQ1000 in [16] is validated through hardware, software and firmware tests. Throughout the development phase of PQ1000, the electrical parameter calibrator Fluke 6100A is used in ECAMEC laboratory. The hardware is developed according to the IEC 61000-4-30 requirements. A series of eleven tests, in accordance with IEC 61000-4-15, is executed. The tests are short term flicker (PST) with square modulation, instant flicker with square modulation, instant flicker with sin modulation, mains frequency variations, second order harmonic influence, linearity evaluation, inter-harmonics pair influence, simultaneous periodical changes of voltage and frequency, fundamental modulation with odd harmonics distortion, flicker caused by phase jump in fundamental, and lastly, flicker present in modulation of 20% duty cycle of the observation period. In short, the first six tests stated above are categorized as performance tests whereas the remaining tests are categorized as influence tests.

Next, time frequency domain method is used in [17] to detect and analyse transient disturbances in voltage supply. The method is enforced in the instrument which consists of voltage transducer, USB DAQ system, phase-locked-loop (PLL) and a computer. Similar to [14] and [15], the software is also programmed using LabVIEW. Before the system is connected to the low voltage distribution system, it is tested by using a programmable AC power source. Different types of test signals are supplied to the instrument for its verification on uninterrupted sampling of the input signal, real time operation, recognition and recording of transient disturbance for different threshold. This particular instrument is then monitored the voltage supply in a low voltage distribution system for three months and the three criteria analysed are peak magnitude, duration and dominant frequency components in the transient signals.

Performance of real time PQA in [18] is analysed. A set of test based on IEC 61000-4-7 is selected, aiming to determine the accuracy of PQA in particular situations. In order to verify the performance of PQA in analysing specific signal generated by non-linear loads or by communication system, three different types of test signals are provided by a signal generator. The first signal composed of a communication signal, with inter-harmonics and two harmonics at different frequency, whereas the second signal consists of combination between communication signal, and two harmonics at different frequency. The combination of the harmonics and inter-harmonics produced by an electronic motor drive, with a communication signal results in the third test signal. Evaluation of the

supplied value and measured value give rise to the accuracy of PQA and thus determine whether PQA complies with the IEC standard or not.

Reference [19] discussed about the implementation of higher-order statistics (HOS) in a virtual instrument for PQ assessment. The introduction of HOS in the PQ measurement algorithms during the last ten years is rather late compared to the other methods like fast Fourier transform (FFT) and wavelet transforms. HOS improved the statistical representation of raw data and subsequently ameliorated the performance of the instrument. The VI is designed in LabVIEW and DAQ NI 6036E is used for acquiring data. Sag, swell and impulsive transients of various parameter settings are simulated through Agilent 6811B AC Power Source/Analyser instrument, with the intention to study the performance of the VI. The adaptability of VI has made it possible to be connected to Agilent DSO6012A digital oscilloscope or even a bigger system with power signal data available.

The number of power system technology research has been increasing due to the extensive usage of computer in power system measurement. The conventional power instruments used for frequency detection and harmonics analysis are not flexible and impracticable for such systems because they are unable to store data for subsequent reference and analysis. The LabVIEW-developed power analyser [20], along with voltage and current sensors, DAQ card and a PC, allows the measurement and analysis of the single phase system parameters. Aside from monitoring various PQ parameters in real time, it provides remote monitoring of the parameters as well. Linear and non-linear load are the two types of load used to test the system performance, where the results obtained are verified with Fluke 43B and Yokogawa CW240. An event logging test has also proved the system ability in detecting and logging the occurrence of PQ events.

Since most of the PQA in the market are quite expensive, a Smart Recording Power Analyser (SRPA) prototype is proposed in [21] to serve as an alternative to those instruments. The analyser, which integrated LabVIEW algorithms with low cost DAQ device, is able to monitor both the numerical data and waveforms during normal operation and also fault condition. The hardware configuration of SRPA consisted of different components, specifically a laptop with LabVIEW installed, NI USB 6212, potential transformers, current transformers, DAQ protection circuit and background noise suppression circuit. SRPA is verified with laboratory-based experiments, where the results

obtained from SRPA and reference measuring tools are compared. In the first experiment, three phase parameters in terms of voltage, current, real power, reactive power, apparent power and power factor are measured from the linear and non-linear load test circuits. Powertek-PX120 power meter is used as the reference measuring equipment in this test. Next, the comparisons of SRPA accuracy in single phase harmonic distortion measurements with the recorded data in Fluke 43B PQA, Yokogawa mixed signal analyser DLM2054 and Chauvin PQA P3945 are performed in the second experiment. Simulated flicker signals of various amplitudes and frequencies are fed to SRPA in the third experiment and its results are then compared with the recommended test condition in IEC 61000-4-15 standard. Besides laboratory testing, SRPA is also tested on-site at 130kW bio-gas pig farm and 1MW solar farm. This is to study its capabilities and functionalities in the real world environment.

The main characteristics of the virtual measurement instrument [22] for detecting and analysing PQ disturbances in a low voltage distribution system are the application of wavelet analysis type on the input signal is dependent on the PQ disturbance studied, wavelet transforms can be applied during real-time or off-line applications, and partial implementation of wavelet transforms for studying the time-frequency characteristics of the input signal frequency band as specified by user. The virtual measurement instrument is made up of a voltage transducer, NI USB 6009 DAQ card, and a laptop with software developed in LabVIEW. The instrument's working mode depends on the PQ disturbance to be identified and studied. Only detection and analysis of transient and stationary or quasi-stationary PQ disturbances have been implemented currently. A single-phase/three-phase programmable power source as well as real voltage signals from the low-voltage distribution system of a building is simulated to test the instrument proposed. Three cases are considered for the testing. First case involves a voltage sag, a voltage swell and a short interruption in voltage supply. A fluctuating harmonic component is analysed with time-frequency analysis in case two whereas voltage notching produced by a six-pulse converter is considered in case three.

There are many sources that can lead to poor quality power supply. The characteristics of single phase induction motor, such as torque requirements and starting current, had been deliberated as one of the contribution towards poor PQ. Therefore, a practical method is employed to mitigate the induction motor PQ problem. The high starting current drawn during motor starting can cause a temporary drop in voltage, which

is also known as voltage sag. The starting current, voltage sag and input current waveform of single phase capacitor run motor are monitored through ammeter, voltmeter and oscilloscope respectively. When the motor is started with different load conditions applied from the electrodynamometer, the measurements from the monitoring equipment differed. The operation of this unmodified motor circuit gives rise to voltage sag of at least 12%. This percentage of voltage sag is reduced to about 9% after adding the capacitor and inductor into the motor circuit [23].

The generation of voltage sag and swell through practical laboratory experiment set up has facilitated the analysis of numerous approaches used for identifying voltage sag and swell in real time. Root mean square, peak, Fourier transform, and missing voltage methods are the four types of algorithms investigated in [24]. In order to study the online performance of these detection methods, a set up consisting of single phase transformer, mechanical relay, induction motor, DAQ card, PC and other components is used to generate and monitor the desired signals. Sag and swell signals are created by changing the tap on the transformer to either a lower or a higher tap depending on the condition of signals wished to be obtained. The voltage output based on the value tapped on the transformer is typically higher or lower than the nominal voltage, therefore the voltage signal is deemed as experiencing sag or swell accordingly.

The relationship between the loads in four different types of full wave rectifier and the harmonic generation is analysed in [25]. The four full wave rectifiers are single phase uncontrolled and controlled rectifiers, three phase uncontrolled and controlled rectifiers, whereas the load connected are either resistive load or resistive-inductive load. Observations of the waveforms have shown that output results are affected by the type of rectifier and load applied. Besides that, the results from Matlab simulation are compared with the ones recorded in the practical set ups. Evidently, the total harmonic distortion (THD) produced by three phase full wave controlled rectifier is the highest among all the rectifiers. High cost of harmonic analyser has led to the Matlab based Simulink model simulation of rectifiers, using the exact parameter from practical experiment, to produce results so that the practical data and simulated data can be compared.

Reference [26] focused on the learning of PQ issues through experimentation. Some of the key issues faced during the automated classification of PQ disturbances are also highlighted by the researchers based on their reviews of the existing works. Instead of

phenomenon based classification, it is suggested that cause based classification should be emphasized for enhancing the comprehension on PQ phenomena. Many classification algorithms have tackled the voltage magnitude events, but that is not the case with transients and harmonics. Since the classification approaches available mainly dealt with single disturbance, the development of multiple disturbance classification is highly recommended. Due to technical and economic constraints, the installation of PQ monitor at all the system nodes is not viable, thus identification of the location and amount of devices to be installed is necessary for the proper monitoring of PQ problems. The effects of possible PQ solutions imposed at every power system levels, ranging from generation to consumer, also have to be evaluated by considering the limitation on technical and economic aspects. The effect of applying two different loads along with star and delta three phase power system connections is investigated in the experiment. Three phase induction motor voltage and current waveforms, as well as their corresponding harmonics and THD are logged continuously with Fluke 434 analyser, starting from before and after the functionalization of motor. Then, the addition of fluorescent lamp into the test circuit has generated more harmonics in the supply.

2.4 Summary and Discussion of the Review

There are many algorithms that can be used for the PQ analysis. Some of the examples mentioned in [3], [15], [19] are wavelet transform, STFT, Gabor transform, S-transform spectrogram, phase-locked-loop-based technique, synchronized rms calculation, and HOS. The PQ monitoring instruments proposed in [3], [14]–[22] are capable of measuring many types of PQ disturbances, with the exception of [17] which only able to detect transient. Several measurement standards, such as IEEE standard 1159-2009, IEC 61000-4-7, IEC 61000-4-15 and IEC 61000-4-30 have been applied in the designing and testing of the systems. The diagnosis results from one or more tests relative to the standards verified that these systems fulfilled the requirements of these standards.

Prior to performance analysis, both hardware and software of the monitoring system need to be developed. The exploitation of sophisticated yet easy to use program, in

this case LabVIEW, has assisted in the development of PQ monitoring software. The hardware design depends on the components chosen. In general, the system consists of three major parts which are input, interfacing device, and displaying unit. At the system input, transducers or step down transformers are used to protect and isolate the DAQ card from the voltage and current measured. The signals measured are then sent to the computer for evaluation in the developed software. Finally, the results comprising of waveforms, measured values and diagnostic parameters are presented on the user interface in computer.

The PQ monitoring instruments can be tested either through laboratory experiment, simulation, or on-site testing. One or more combinations of testing are applied by the researchers in [3], [14]–[22] for verifying the competency of their works. Majority of these researchers have set up the laboratory experiments to examine their system based on the signals produced by the laboratory equipment. In simulation verification mode, the signals are injected to the system through the programmable Agilent 6811B AC Power Source/Analyser [19] and IPC [4]. There are also some researchers, for example [16], [18], and [22], who have tested their projects through on-site testing with the intention to study the system endurance in real world situations. Some of the experiments for voltage sag and harmonic distortion are discussed in [23]–[26].

The data collection from the reference meters and PQ monitoring instruments proposed are required for the assessment and comparison purposes. Examples of standard meter used in [14], [16], [20], [21] are Fluke 1745 series three-phase PQ loggers memobox, Fluke 6100A, Fluke 43B, Yokogawa CW240, Powertek-PX120 power meter, Yokogawa DLM2054, and Chauvin PQA P3945. Accuracy and efficiency of the proposed system are computed by comparing the supplied value with the measured value obtained through a series of testing. If the value analyzed fall in the range permitted by the standards, then the system's standard compliance is justified.

This project will be focusing on the performance analysis of the system developed in [3] through several experiment set ups modified from [23]–[26]. The reference tool chosen is Fluke 43B PQA. Since Fluke 43B PQA is compliant to IEC 61000-4-30 Class A, in case the value measured by PQMS is comparable to the value measured by PQA, then PQMS is comply with the standard too.

CHAPTER 3

METHODOLOGY

3.1 Introduction

Before the commencement of PQMS testing, the instrument needs to be developed first. The hardware and software development of PQMS are not included in the scope of this project because it has been completed by other researchers prior to this project. However, the next subsection gives a brief overview on the components of this instrument.

The backbones of this project are the various experiments used for validating the PQMS performance. Through these experiments, the capability of PQMS in measuring and detecting PQ problems are examined and analysed by referring to Fluke 43B PQA. A total of five different experiment set ups inclusive of three phase squirrel cage induction motor no load test, blocked rotor test, voltage sag and harmonic experiments, voltage sag experiment from single phase capacitor run motors, and single phase full wave controlled rectifier have been conducted in various laboratories in FKE, UTeM with the purpose of achieving the project objectives.

3.2 Components in Power Quality Monitoring System

Figure 3.1 depicts the block diagram of real time PQMS [3]. PQMS is made up of four main components, voltage transducer, current transducer, NI USB 6009 DAQ card and a tablet installed with the PQ monitoring software which is developed in Microsoft Visual Basic 6.0.

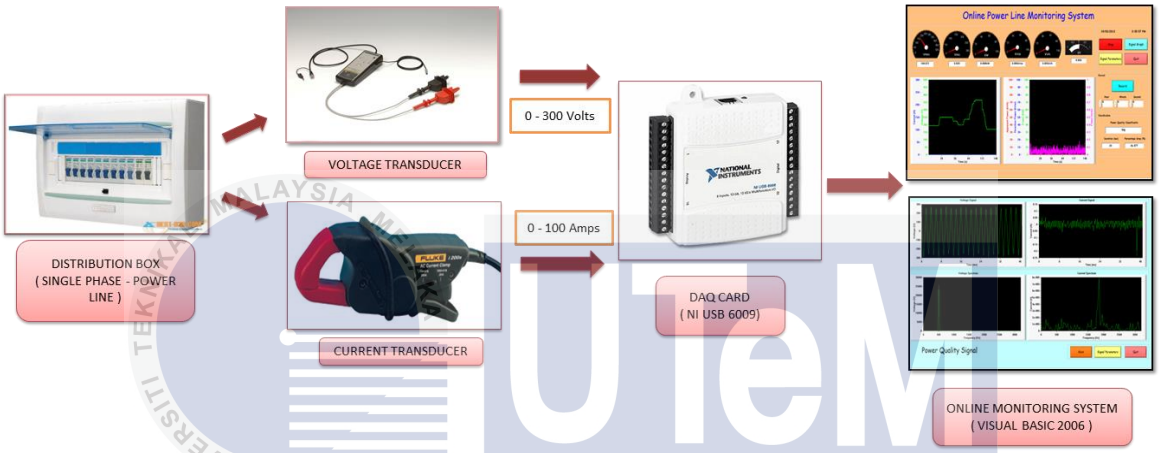

Figure 3.1: Block Diagram of Real Time Power Quality Monitoring System

The transducers act as an input to the NI USB 6009 DAQ card. The card is interfaced with the Visual Basic software and the output is displayed on the Graphical User Interface (GUI) developed in Visual Basic software. The system range of measurement for voltage and current are 0-300V and 0-100A respectively. Since NI USB 6009 operating inputs are 5V and 200mA, transducers are used to step down the input voltage and current, so that the DAQ card will not be damaged. Signals received or measured are then integrated and the signals or data are sent into computer.

3.3 Technique Overview

Two types of laboratory experiment are employed for the PQMS testing. They are power system measurements and PQ event identification. Extensive evaluation of the system performance is possible due to the utilization of PQA and PQMS in collecting the data from these experiments.

3.3.1 Power System Measurement

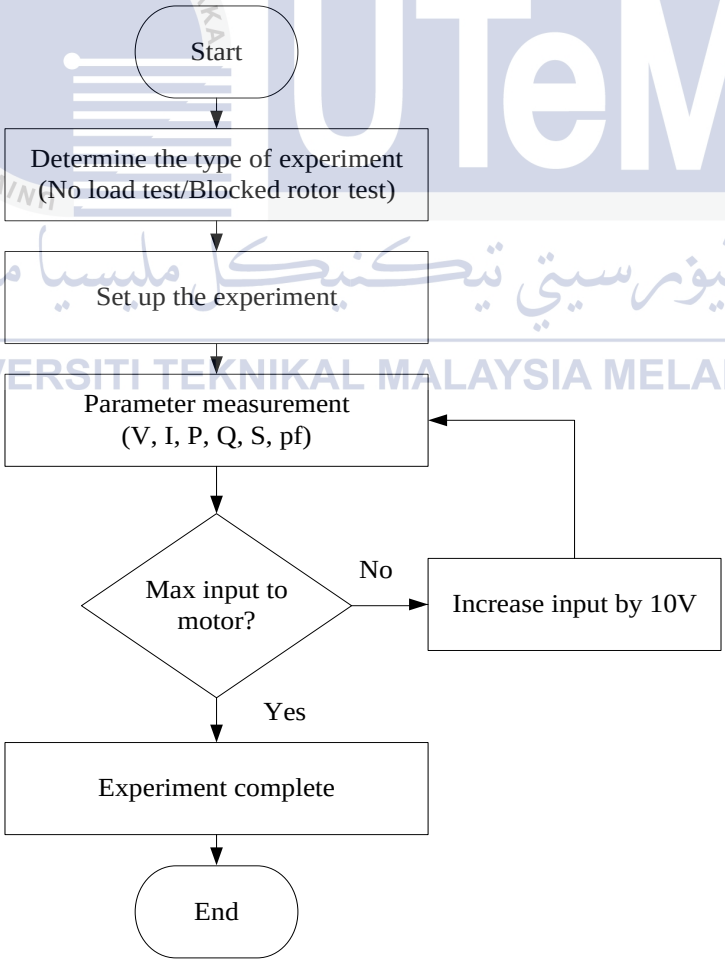

Figure 3.2: Flowchart of Experiment Implemented for Measurement

Since the three phase squirrel cage induction motor no load test and blocked rotor test are intended for measuring the power system parameters, the process flow of the experiments is illustrated in Figure 3.2. Firstly, the type of experiment to be used, either no load test or blocked rotor test, is decided before setting up the experiment according to the block diagram in section 3.4. Repeated measurements of the parameters identified are performed with the aid of PQA and PQMS until reaching the maximum allowable motor input. The validation of the results through APE enables the analysis on the PQMS performance.

3.3.2 Power Quality Event Identification

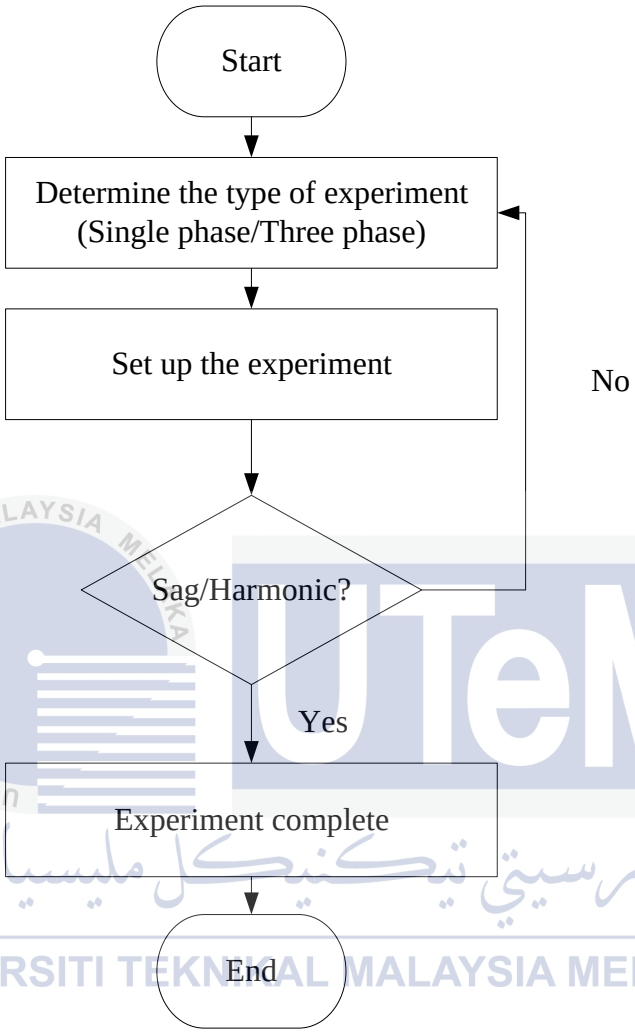

Figure 3.3: Flowchart of Experiment Implemented for Power Quality Event Identification

Figure 3.3 discloses the flowchart of a PQ disturbance experiment. There are four types of experiments in this category, for instance, single phase voltage sag and harmonic distortion, as well as three phase voltage sag and harmonic distortion. Two types of set up are used in the single phase experiment, whereas there is only one experiment for the three phase experiment. Similarly, the circuit connections for all these experiments are based upon the block diagram in section 3.4. The experiment is considered to be successful when the PQMS classification of disturbance matches the PQ event created by experiment.

3.3.3 Reference Instrument

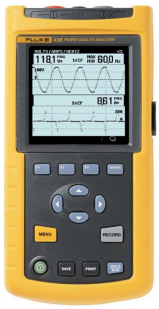

Figure 3.4: Power Quality Analyser

Figure 3.4 displays the Fluke 43B PQA [27] used in the project. It can function as a PQA, multimeter or oscilloscope. To be exact, this PQA is capable of measuring voltage, current, frequency, power, sags and swells, inrush current, transients, resistance, continuity, capacitance, temperature and harmonics. The signal waveform also can be shown on the screen of the PQA. Furthermore, the recording function available ease the data collection process, where one does not need to be present at all times to collect the data. As long power is supplied to the meter, either on battery or plugged in, the device can record the selected parameter up to 16 days. For instance, one wished to monitor the supply fluctuation that happened in a system, this can be done through the 'sags & swells' function of PQA, where it can record the voltage and current fluctuation for a specific time. After the data is recorded, it can be saved into one of the 20 memory slots provided by PQA. If all the memory slots are occupied, the new data will overwrite the content in memory slot 1 and so on. The data saved can then be recalled in the PQA itself or transferred to a computer through an USB interface cable. FlukeView software must be installed in the computer beforehand performing the data transfer.

3.4 Description of Work

The experimental set ups used in the project are deliberated in the sequence of three phase squirrel cage induction motor no load test and blocked rotor test for measuring the six parameters concerned, capacitor run motors set ups with different load condition for generating single phase voltage sag, full wave controlled rectifier for generating single phase harmonic distortion, and finally the three phase induction motor with transformer for generating three phase voltage sag and harmonic distortion.

Absolute percent error (APE) in equation 3.1 conveyed the deviation of PQMS results acting as the recorded value in the equation from the true value measured by PQA.

$$APE = \left|\frac{Recorded\ value - True\ value}{True\ value}\right| \times 100\% \quad (3.1)$$

The calculation of mean APE is based upon equation 3.2. It is useful in validating the accuracy of PQMS measurements as it denotes the average APE of a parameter.

$$Mean\ APE = \frac{Total\ APE}{Total\ number\ of\ measurements} \quad (3.2)$$

Calculation of voltage drop is essential for validating the voltage sag occurrence. The application of voltage before and during the sag as the initial and final voltage in the equation 3.3 provides the percentage of voltage drop. An event can be classified as voltage sag if and only if the percentage of voltage drop is more than 10%.

$$Voltage\ drop\ (\%) = \left|\frac{Initial\ voltage - Final\ voltage}{Initial\ voltage}\right| \times 100\% \quad (3.3)$$

3.4.1 Three Phase Squirrel Cage Induction Motor No Load Test

A no load test for three phase squirrel cage induction motor, which aimed to test the accuracy of PQMS in measurement, is conducted in Makmal Mesin 1, FKE, UTeM. Single phase circuit is unfavorable as its maximum voltage supply is only 240V.

No load test [28] is one of the three tests that can be used to determine the circuit model parameter to be used in the equivalent circuit of an induction motor. The other two being blocked rotor test and DC test for stator resistance. In this test, rotational losses of the motor are measured and information about its magnetization current can be obtained. But in this project, these parameters and information are not the main concern. The only concern is voltage, current, real power, reactive power, apparent power and power factor that can be produced by the motor. Table 3.1 shows the induction motor rating, as specified on its nameplate. Figure 3.5 gives an overview on the simplified circuit connection for a three phase induction motor no load test.

Table 3.1: Specifications for Three Phase Squirrel Cage Motor

Voltage	220/380 V Δ/Y
Current	4.7/2.7 A Δ/Y
Power	1100 W
Power Factor	0.8
Speed	2800 rpm
Frequency	50 Hz

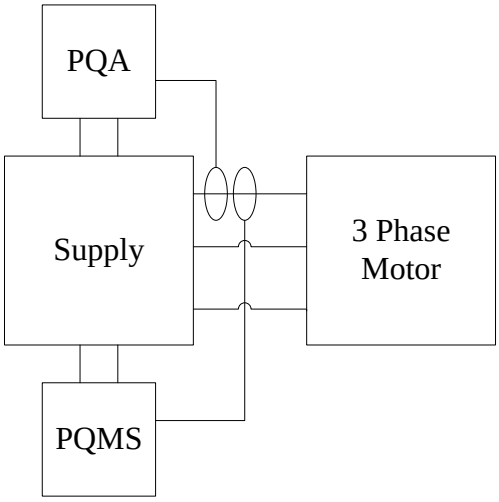

Figure 3.5: Block Diagram for No Load Test

The connection in Figure 3.6 is exactly the same as the one shown in Figure 3.5. During the experiment, after each measurement, the input is increased by 10V and the motor outputs, in terms of voltage, current, real power, reactive power, apparent power and power factor, are measured with PQA and PQMS. The application of these results for the APE calculation as defined in equation 3.1 permits the authentication of the PQMS operation. Equation 3.2 is used to compute the mean APE of each parameter.

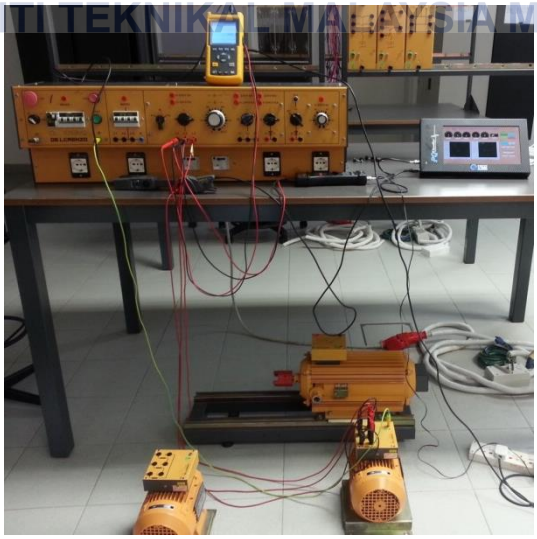

Figure 3.6: Experimental Set Up for No Load Test

3.4.2 Three Phase Squirrel Cage Induction Motor Blocked Rotor Test

Besides no load test of three phase squirrel cage induction motor, blocked rotor test is also chosen for testing the capability of PQMS in taking measurement. Figure 3.7 displays the block diagram of the experiment. The motor used for testing is the same three phase squirrel cage induction motor as in no load test. In this test, the rotor is stalled because it is blocked with a DC voltage-supplied electromagnetic brake. Three phase AC supply is applied instead to the star-connected stator winding of the motor. Then, PQA and PQMS are connected to the AC supply for voltage and current measurements.

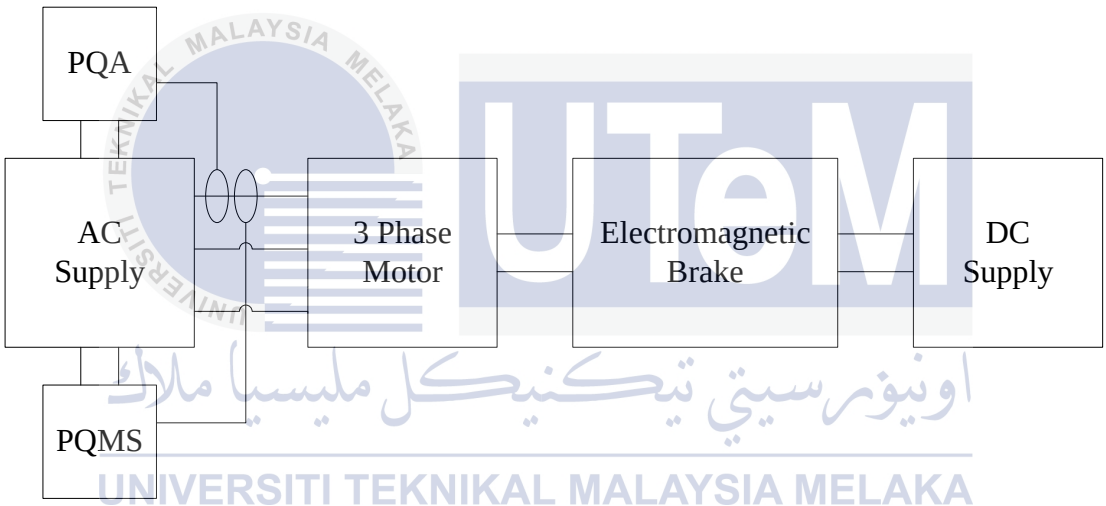

Figure 3.7: Block Diagram of Blocked Rotor Test

The experimental set up in Makmal Mesin Elektrik 1, FKE, UTeM is depicted in Figure 3.8. After the voltage is supplied to both motor and brake, the six parameters concerned, namely voltage, current, real power, reactive power, apparent power and power factor are measured. The AC supply is then increased by 10V and the measurements are repeated. Data collection for each parameter is analysed by using equation 3.1 to calculate the APE for every measurement. The mean APE of each parameter is also determined by considering all the APE for that particular parameter, as in equation 3.2.

Figure 3.8: Experimental Set Up for Blocked Rotor Test

3.4.3 Single Phase Voltage Sag

There are two types of load condition in accomplishing the single phase voltage sag experiment as concisely discussed below. When there is only motor present in the load, six motors are necessary as the voltage drop in a single motor is not large enough to be identified as voltage sag.

Case 1: Motor Only

The block diagram of the voltage sag experiment is illustrated in Figure 3.9. The connection of measuring instruments is such that they can capture the voltage sag signal occurring at supply during the motor starting. The sag & swell function accessible through the main menu of PQA is used to record the phenomena.

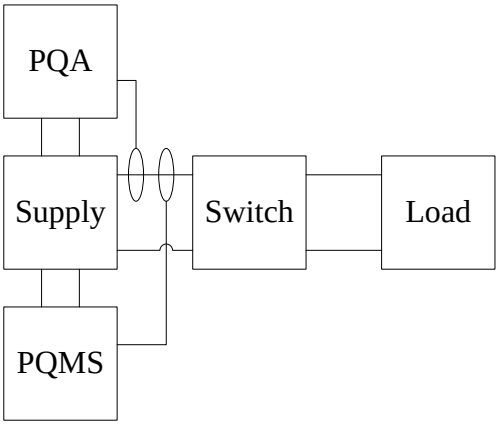

Figure 3.9: Block Diagram for Single Phase Voltage Sag Experiment

Figure 3.10 presents the schematic diagram of the experiment. All the motors are connected in parallel to the variable AC voltage source, where the source is adjusted and fixed to 240V throughout the experiment. Transmission line module of zero resistance is used as the switch for the circuit, so that the electricity does not flow through the motors once the supply is turned on. Each motor is coupled to a dynamometer and each dynamometer is powered with $24V_{dc}$ accordingly. The coupling is done by using a timing belt. All the dynamometers are adjusted to minimum load, i.e. by turning the control knob of the dynamometer fully anti-clockwise. The experimental set up in Makmal Teknologi Elektrik, FKE, UTeM is shown in Figure 3.11.

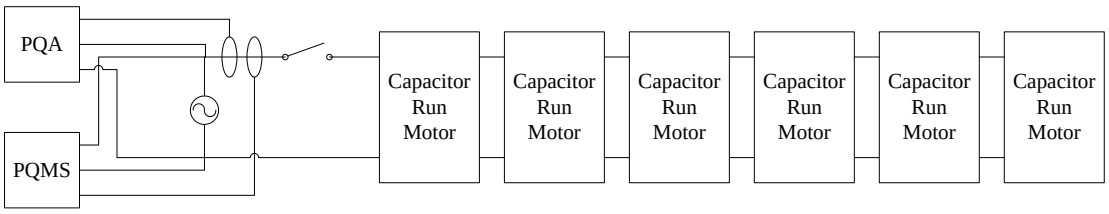

Figure 3.10: Schematic Diagram of the Experiment

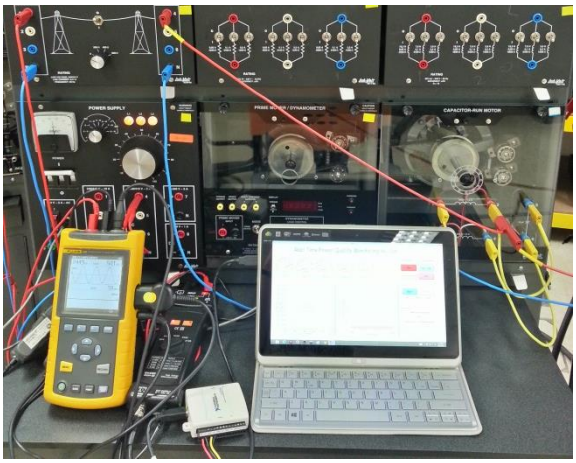

Figure 3.11: Practical Set Up for the Experiment

The specifications of the capacitor run motors and dynamometers used are tabulated in Table 3.2 and Table 3.3 respectively.

Table 3.2: Specifications of Capacitor Run Motor

Output	175 W
Rated Speed	1415 rpm
Rated Voltage	240 V
Full Load Current	1.15 A
Frequency	1 ~ 50 Hz

Table 3.3: Specifications of Dynamometer

Input	24 V_{dc}
Output	175 W
Rated Speed	0 – 2500 rpm
Rated Torque	0 – 3 Nm

Case 2: Motor and RLC Load

The experiment is then modified by adding RLC load in parallel with the capacitor run motors. Four stations with four motors and RLC loads are used instead of six motors and the procedure is the same as the previous experiment. Block diagram and practical set up of the experiment are represented in Figure 3.12 and Figure 3.13 respectively.

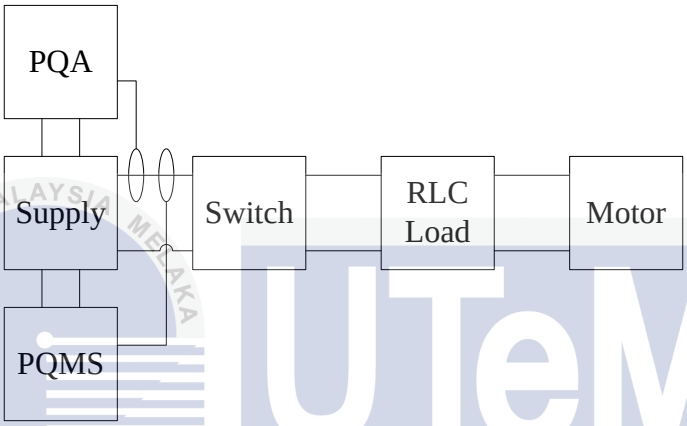

Figure 3.12: Block Diagram of the Experiment

Figure 3.13: Practical Set Up for Voltage Sag Experiment with Combination of Motor and RLC Load

3.4.4 Single Phase Full Wave Controlled Rectifier

In order to obtain the harmonic signal, full wave controlled rectifier with parallel connection of RLC load is constructed in Makmal Elektronik Kuasa, FKE, UTeM. The block diagram for the experiment is disclosed in Figure 3.14. The whole system, which consists of power thyristors and RLC load, is connected in parallel and powered through $240V_{ac}$ variable voltage supply. The supply is adjusted and maintained at 240V throughout the experiment. Similar with other experiments in this project, both PQA and PQMS are used for the harmonics measurement.

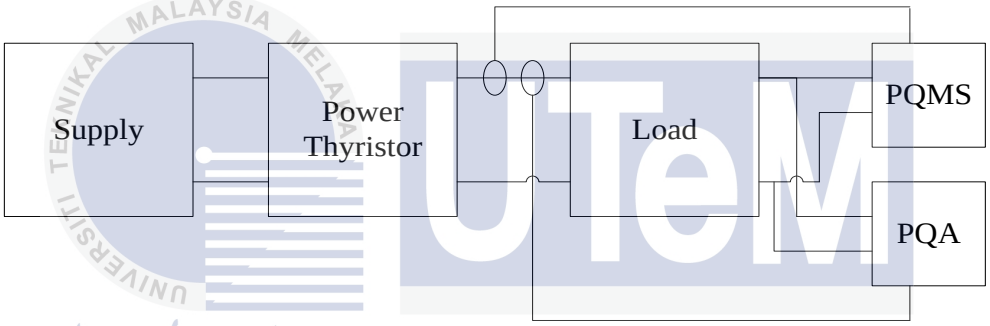

Figure 3.14: Block Diagram for Full Wave Controlled Rectifier Experiment

Figure 3.15 reveals the experimental set up for full wave controlled rectifier. The firing angle of thyristors is adjustable through the controller connected to the power thyristor module. Initially, all the loads and controller angle are set to zero. After switching on the supply along with adjusting to the desired firing angle, load is inserted with precaution so that the voltage is above 216V and the current is lower than 1A. This is because any voltage lower than 216V will be classified as voltage sag.

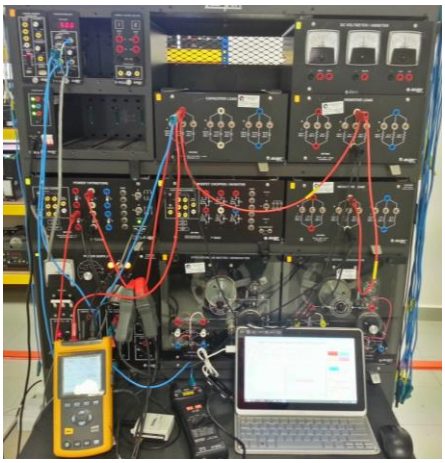

Figure 3.15: Experimental Set Up for Full Wave Controlled Rectifier

3.4.5 Three Phase Squirrel Cage Induction Motor Voltage Sag and Harmonic Distortion

In this experiment, three phase squirrel cage motor is used for the purpose of obtaining the voltage sag and harmonic signals. The input of star-star (Y-Y) transformer is connected to the supply while the transformer output is connected to the star-delta motor starter, where the motor starter served as a switch to turn on or off the three phase motor. The desired signals, for instance voltage sag and harmonic signals are acquired with PQA and PQMS at the supply terminals. Figure 3.16 represents the experiment set up in the form of block diagram whereas Figure 3.17 shows the practical set up in the laboratory.

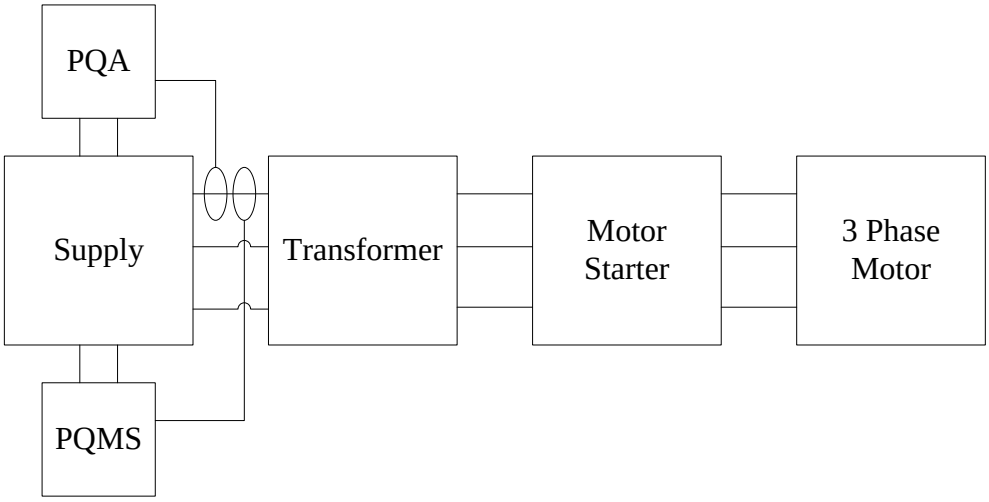

Figure 3.16: Block Diagram of Experiment

Figure 3.17: Experimental Set Up for Three Phase Motor

In order to power up the circuit, variable three phase power supply is adjusted to 240V_{L-L} and fixed to this voltage throughout the experiment. At the beginning of experiment, the motor did not function after activating the supply because motor starter is not initiated yet. At this point, PQA and PQMS had begun to record the signals from the supply.

CHAPTER 4

RESULTS AND DISCUSSION

4.1 Introduction

The performance of PQMS is analyzed with the results collected from a number of experiments. In comparisons of the results collected from PQA and PQMS, the proposed system performance in terms of measurements and PQ problem classifications are evaluated extensively. The utilization of no load test and blocked rotor test of a three phase squirrel cage induction motor has prompted the parameter measurement assessments. Data from these two experiments are enumerated into twelve different tables and APE is calculated for every measurement of the six different parameters, for instance voltage, current, real power, reactive power, apparent power, and power factor.

Besides the parameter measurements, the ability of PQMS in detecting PQ problems is also tested. In this project, only voltage sag and harmonic distortion in both single phase and three phase loads are considered. Voltage sag is observed during the starting up of six single phase capacitor run motors, four single phase capacitor run motors with RLC load, and three phase induction motor, whereas harmonic distortion is observed from the single phase full wave controlled rectifier with RLC load, and three phase induction motor. The implementation of distinctive loads in each set up has resulted in the PQ disturbances mentioned. The system performance is then analyzed through the data available in the screenshots of PQA and PQMS.

4.2 Performance of PQMS

Six motor parameters are collected each from the execution of two different experiments on a three phase squirrel cage induction motor, whereby no load test and blocked rotor test are chosen to examine the PQMS performance. The comparisons between the data collected using PQA and PQMS yielded the APE and average APE, which eventually clarify the efficiency of PQMS. Graphs are also plotted to give a sophisticated interpretation on the data collection.

4.2.1 No Load Test

Both PQA and PQMS measured the motor parameters comprising of voltage, current, real power, reactive power, apparent power and power factor. All the measurements for no load test are listed in Table 4.1 to Table 4.6, where each table corresponded to one of the motor parameters. Better illustrations of the data collection which differentiate the PQA and PQMS performance are represented in Figure 4.1 and Figure 4.2.

Table 4.1: Voltage Measured from No Load Test

Measurement	PQA (V)	PQMS (V)	APE (%)
1	30.89	30.88	0.032
2	40.4	40.4	0.000
3	50.39	50.34	0.099
4	60.1	60.1	0.000
5	70.3	70.23	0.100
6	80.2	80.2	0.000
7	90.4	90.44	0.044
8	100.5	100.52	0.020
9	109.8	109.85	0.046
10	121.3	121.41	0.091
11	130.2	130.27	0.054
12	140.6	140.61	0.007
13	150.8	150.79	0.007
14	160.7	160.76	0.037
15	170.2	170.22	0.012
16	180.8	180.84	0.022
17	190.7	190.73	0.016
18	200.9	200.85	0.025
19	210.5	210.5	0.000
20	220.1	220.11	0.005
21	230.2	230.15	0.022
22	240.1	240.12	0.008
23	250.2	250.23	0.012
24	260.4	260.45	0.019
25	271	271	0.000
26	280.5	280.5	0.000
27	290.2	290.22	0.007
28	300	300.05	0.017
Mean APE			0.025

Table 4.2: Current Measured from No Load Test

Measurement	PQA (A)	PQMS (A)	APE (%)
1	1.06	1.06	0.000
2	0.8	0.8	0.000
3	0.72	0.72	0.000
4	0.64	0.64	0.000
5	0.68	0.68	0.000
6	0.71	0.71	0.000
7	0.76	0.76	0.000
8	0.81	0.81	0.000
9	0.91	0.91	0.000
10	0.97	0.97	0.000
11	1.07	1.07	0.000
12	1.19	1.19	0.000
13	1.32	1.32	0.000
14	1.44	1.44	0.000
15	1.58	1.58	0.000
16	1.76	1.77	0.568
17	1.95	1.95	0.000
18	2.2	2.21	0.455
19	2.51	2.51	0.000
20	2.9	2.91	0.345
21	3.41	3.41	0.000
22	3.95	3.95	0.000
23	4.38	4.38	0.000
24	4.81	4.81	0.000
25	5.16	5.16	0.000
26	5.51	5.51	0.000
27	5.84	5.84	0.000
28	6.25	6.25	0.000
Mean APE			0.049

Table 4.3: Real Power Measured from No Load Test

Measurement	PQA (W)	PQMS (W)	APE (%)
1	32	32	0.000
2	32	32	0.000
3	36	36	0.000
4	38	38	0.000
5	45	45	0.000
6	52	52	0.000
7	60	60	0.000
8	70	70	0.000
9	78	78	0.000
10	87	87	0.000
11	103	103	0.000
12	125	125	0.000
13	137	137	0.000
14	160	160	0.000
15	177	177	0.000
16	204	204	0.000
17	245	245	0.000
18	278	279	0.360
19	326	326	0.000
20	382	383	0.262
21	459	459	0.000
22	550	550	0.000
23	640	640	0.000
24	728	730	0.275
25	783	783	0.000
26	850	849	0.118
27	932	932	0.000
28	1013	1013	0.000
Mean APE			0.036

Table 4.4: Reactive Power Measured from No Load Test

Measurement	PQA (VAR)	PQMS (VAR)	APE (%)
1	4	4	0.000
2	5	5	0.000
3	1	1	0.000
4	8	8	0.000
5	15	15	0.000
6	25	25	0.000
7	35	35	0.000
8	46	46	0.000
9	61	61	0.000
10	78	78	0.000
11	98	98	0.000
12	118	118	0.000
13	145	145	0.000
14	176	176	0.000
15	210	211	0.476
16	246	247	0.407
17	290	290	0.000
18	345	345	0.000
19	420	420	0.000
20	511	511	0.000
21	636	636	0.000
22	768	768	0.000
23	920	921	0.109
24	1048	1049	0.095
25	1161	1161	0.000
26	1290	1289	0.078
27	1424	1424	0.000
28	1575	1575	0.000
Mean APE			0.042

Table 4.5: Apparent Power Measured from No Load Test

Measurement	PQA (VA)	PQMS (VA)	APE (%)
1	32	32	0.000
2	32	32	0.000
3	36	36	0.000
4	38	38	0.000
5	47	47	0.000
6	56	56	0.000
7	68	68	0.000
8	81	81	0.000
9	98	98	0.000
10	117	117	0.000
11	139	139	0.000
12	167	167	0.000
13	199	199	0.000
14	231	231	0.000
15	269	269	0.000
16	319	320	0.313
17	372	372	0.000
18	441	442	0.227
19	549	549	0.000
20	638	640	0.313
21	779	780	0.128
22	948	948	0.000
23	1122	1123	0.089
24	1278	1280	0.156
25	1398	1398	0.000
26	1545	1544	0.065
27	1695	1695	0.000
28	1875	1876	0.053
Mean APE			0.048

Table 4.6: Power Factor Measured from No Load Test

Measurement	PQA	PQMS	APE (%)
1	0.99	0.99	0
2	0.99	0.99	0
3	1	1	0
4	0.98	0.98	0
5	0.95	0.95	0
6	0.9	0.9	0
7	0.86	0.86	0
8	0.82	0.82	0
9	0.79	0.79	0
10	0.75	0.75	0
11	0.71	0.71	0
12	0.71	0.71	0
13	0.68	0.68	0
14	0.65	0.65	0
15	0.64	0.64	0
16	0.64	0.64	0
17	0.62	0.62	0
18	0.62	0.62	0
19	0.6	0.6	0
20	0.6	0.6	0
21	0.59	0.59	0
22	0.58	0.58	0
23	0.57	0.57	0
24	0.57	0.57	0
25	0.56	0.56	0
26	0.55	0.55	0
27	0.55	0.55	0
28	0.54	0.54	0
Mean APE			0

Voltage data from the no load test is tabulated in Table 4.1. An increment of almost 10V per measurement is observed for the values recorded by PQA and PQMS. Six out of the twenty-eight measurements, particularly the 2nd, 4th, 6th, 19th, 25th and 26th measurement gave an APE of 0% denoted the same value recorded for both PQA and PQMS. The rest of the measurements have APEs ranged from 0.005% to 0.1%. These 28 APEs resulted in a mean APE of 0.025%.

Current has declined from 1.06A to 0.8A and the decrement continued at a rate of 0.8A until 0.64A in the 4th measurement. It is then gradually increased to 6.25A in the 28th measurement. Only three measurements in Table 4.2 showed different values for PQA and PQMS, which are 16th measurement (0.568%), 18th measurement (0.455%) and 20th measurement (0.345%). A mean APE of 0.049% is obtained with all the measurement APEs considered.

Table 4.3 shows the real power measured by PQA and PQMS, where the values recorded are within the range of 32W to 1013W. There are 4 measurements, which have APE other than 0%. For instance, the APE for 18th, 20th, 24th and 26th measurements are 0.36%, 0.262%, 0.275% and 0.118% respectively. Meanwhile, the rest of the measurements engender APE of 0%. Consequently, mean APE of 0.036% is attained with the consideration of 28 APEs.

A mean APE of 0.042% is obtained for the reactive power measurements. In the data recorded for reactive power, as tabulated in Table 4.4, most of the measurements recorded by PQA and PQMS demonstrate no deviation, except for 15th, 16th, 23rd, 24th, and 26th measurement. The APE for these 5 measurements is ranged from 0.078% to 0.476%. Although a decreasing trend is observed in the first three measurements, the next twenty-five measurements presented a constant growth in value until it reaches 1575VAR in the 28th measurement.

The representation of apparent power in Table 4.5 exhibits an ascending progression. Similar like the other 4 parameters recorded earlier, there are some discrepancies in values recorded by the instruments and these differences give rise to APE ranging from 0.053% to 0.313%. The mean APE calculated for this parameter is 0.048%, taking into account all the 28 measurements, including the 8 measurements that recorded certain percentage of APE.

Initially, the power factor in Table 4.6 is almost unity in the first three measurements, then it started to drop from the 4th measurement onwards. The mean APE for power factor is 0% as it is the only parameter that recorded 0% APE for every measurement.

Table 4.7: Mean APE and Range of APE for Each Parameter

APE / Parameter	Lowest	Highest	Mean
Voltage	0	0.1	0.025
Current	0	0.568	0.049
Real Power	0	0.360	0.036
Reactive Power	0	0.476	0.042
Apparent Power	0	0.313	0.048
Power Factor	0	0	0

The range of APE for each parameter is summarized in Table 4.7. It is clear that every parameter recorded 0% APE as their lowest APE, but they showed different value of highest APE. Among all the parameters, current has the highest value of APE, which is 0.568%, then followed by reactive power (0.476%), real power (0.36%), apparent power (0.313%), voltage (0.1%) and power factor (0%). Although the APE calculated for some parameter is quite high, but the mean APE for all the parameter is less than 0.05%. The low percentage of mean APE proved the close resemblance of the value measured by PQMS with that of PQA, thus indicating the system proposed is indeed efficient.

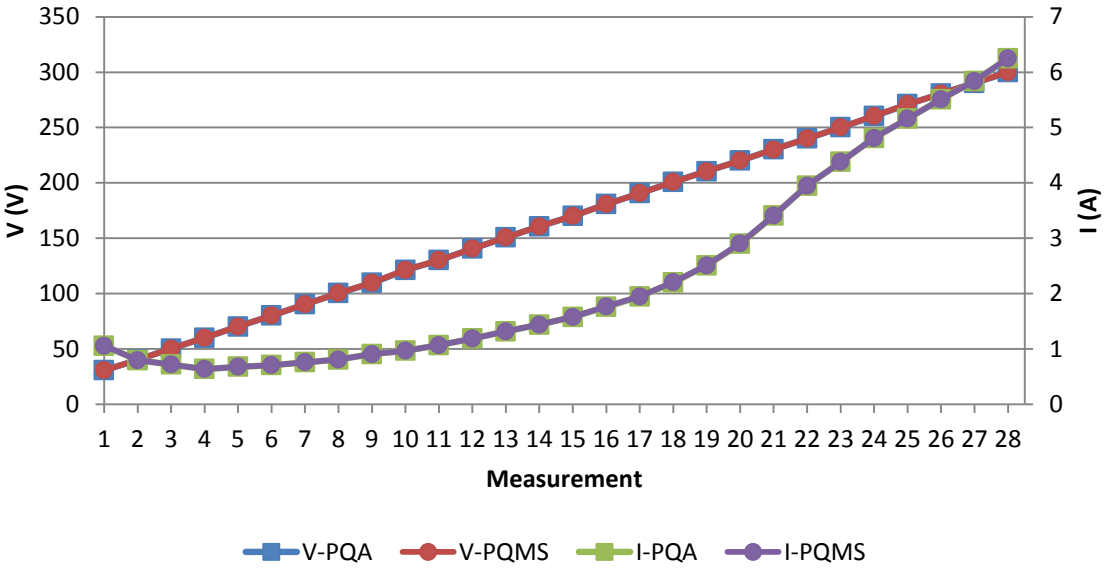

Figure 4.1: Graph of Voltage and Current Measured by PQA and PQMS

Since the value of voltage and current differ greatly, the parameters are plotted on two different axes in Figure 4.1. The voltage of PQA increased linearly from 30V in 1st measurement to 300V in 28th measurement. Likewise, the voltage measured by PQMS also portrayed linear increment from the 1st to the last measurement. In fact, the voltage lines overlapped due to the similarity in values measured by PQA and PQMS. The voltage increased gradually as a result of increasing the motor supply by 10V after each measurement. As for current measured by both PQA and PQMS, the small deviation in current values has also instigated the overlapping of PQA and PQMS data series. The initial current value was 1.06A for both and they started to decline from 0.8A in 2nd measurement to 0.68A in 5th measurement. Then, the current heightened in a steady trend until the 20th measurement of 2.9A for PQA and 2.91A for PQMS. After that particular measurement, they tended to escalate in a much steeper manner for the rest of the measurements. When more voltage is supplied, the motor starts to rotate faster, thus the current drawn by motor also increases.

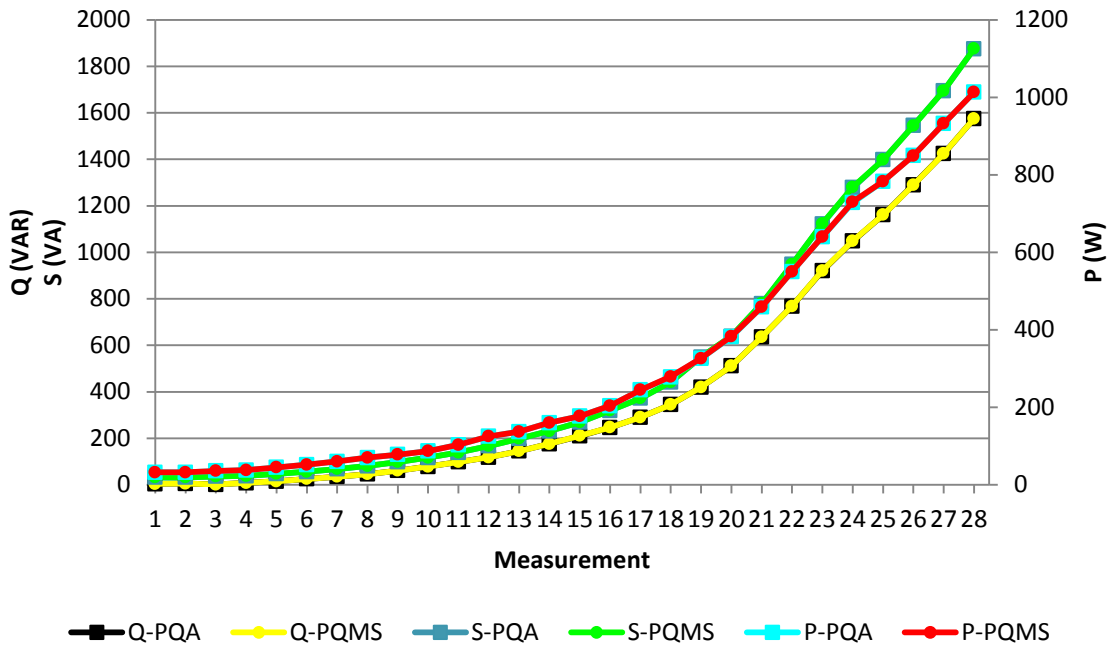

Figure 4.2: Graph of Real Power, Reactive Power, Apparent Power Measured by PQA and PQMS

Figure 4.2 illustrates the graph for real power (P), reactive power (Q), and apparent power (S) measured by PQA and PQMS. All parameters are shown to increase exponentially. These three parameters exhibit similar rising pattern because they are related by power factor. From graph, real power swell steadily until the 24th measurement, henceforth the gradient of increment is lowered slightly. The value measured by PQA and PQMS on the 24th measurement are 728W and 730W respectively. Both reactive power and apparent power ascend in a comparable style with real power without suffering the slight drop in gradient at the 24th measurement. The initial divergence between reactive power and apparent power are small, but it starts to increase from the 12th measurement onwards. They are separated by a difference of 49 at the 12th measurement, and this gap intensified to 300 at the 28th measurement. It is noticed that real power intersected the apparent power from 19th to 21st measurement.

4.2.2 Blocked Rotor Test

The parameters and data interpretation are analogous to the no load test. Table 4.8 to Table 4.13 organized the six different motor parameters, i.e. voltage, current, real power, reactive power, apparent power and power factor, in which each parameter consists of 18 measurements. The utilization of equation 3.1 and 3.2 along with the data collected signifies the accuracy of PQMS in taking measurements. Since the measurement of PQA and PQMS deviated in a small percentage, distinctive line styles are essential for the differentiation of PQA and PQMS data series in Figure 4.3 and Figure 4.4 so that each data trend is perceptible.

Table 4.8: Voltage Measured from Blocked Rotor Test

Measurement	PQA (V)	PQMS (V)	APE (%)
1	30.07	30.07	0.000
2	40.01	40.02	0.025
3	50.51	50.52	0.020
4	60.7	60.72	0.033
5	70.1	70.06	0.057
6	80.5	80.46	0.050
7	90.8	90.83	0.033
8	100.3	100.32	0.020
9	110.6	110.66	0.054
10	120.5	120.56	0.050
11	130.9	130.8	0.076
12	140.8	140.85	0.036
13	150.1	150.12	0.013
14	160.1	160.16	0.037
15	170.9	170.93	0.018
16	180.5	180.54	0.022
17	190.3	190.21	0.047
18	200.1	200.23	0.065
Mean APE			0.036

There is only one measurement that gives an APE of 0% in Table 4.8. A difference between 0.01V and 0.13V in the PQA and PQMS voltage measurement caused the APE for 2nd until 18th measurement to range from 0.013% to 0.076%. Overall, the PQMS measurement diverged from PQA by 0.036%.

Table 4.9: Current Measured from Blocked Rotor Test

Measurement	PQA (A)	PQMS (A)	APE (%)
1	0.80	0.80	0.000
2	1.11	1.11	0.000
3	1.43	1.43	0.000
4	1.76	1.76	0.000
5	2.06	2.06	0.000
6	2.35	2.35	0.000
7	2.69	2.69	0.000
8	2.94	2.94	0.000
9	3.22	3.21	0.311
10	3.47	3.47	0.000
11	3.72	3.72	0.000
12	3.86	3.86	0.000
13	3.97	3.97	0.000
14	4.06	4.07	0.246
15	3.99	4.00	0.251
16	2.54	2.54	0.000
17	2.26	2.26	0.000
18	2.06	2.06	0.000
Mean APE			0.045

In Table 4.9, there are 3 measurements with APE greater than 0%. A non-zero APE is gained for a 0.01A variance in PQA and PQMS measurement. In precise, they are 0.311%, 0.246% and 0.251% for the 9th, 14th and 15th measurement respectively. Because of that, the resulted mean APE for current is 0.045%.

Table 4.10: Real Power Measured from Blocked Rotor Test

Measurement	PQA (W)	PQMS (W)	APE (%)
1	24	24	0.000
2	44	44	0.000
3	72	72	0.000
4	107	107	0.000
5	144	144	0.000
6	189	189	0.000
7	243	243	0.000
8	295	295	0.000
9	353	352	0.283
10	413	414	0.242
11	482	482	0.000
12	538	538	0.000
13	590	590	0.000
14	638	639	0.157
15	668	668	0.000
16	431	431	0.000
17	404	404	0.000
18	388	388	0.000
Mean APE			0.038

Out of 18 measurements in Table 4.10, 15 achieved 0% APE denoting equal measurement for PQA and PQMS. The remaining 3 measurements are the 9th measurement with APE of 0.283%, 10th measurement with APE of 0.242% and 14th measurement with APE of 0.157%. The presence of 1W difference in these measurements introduced diminishing APE as the level of measurement increased. Subsequently, a mean APE of 0.038% is acquired with the consideration of all the APEs for real power.

Table 4.11: Reactive Power Measured from Blocked Rotor Test

Measurement	PQA (VAR)	PQMS (VAR)	APE (%)
1	1	1	0.000
2	2	2	0.000
3	4	4	0.000
4	8	8	0.000
5	10	10	0.000
6	14	14	0.000
7	21	21	0.000
8	26	26	0.000
9	36	36	0.000
10	47	47	0.000
11	61	61	0.000
12	77	77	0.000
13	96	96	0.000
14	119	120	0.840
15	149	149	0.000
16	150	150	0.000
17	149	149	0.000
18	141	141	0.000
Mean APE			0.047

Contrasting from the previous findings in Table 4.8 to Table 4.10, only the 14th measurement, which differed by 1VAR, recorded an APE of 0.840% successively. In spite of the existence of APE in the 14th measurement of Table 4.11, the resulting mean APE is 0.047% due to 0% APE contribution by the other 17 measurements.

Table 4.12: Apparent Power Measured from Blocked Rotor Test

Measurement	PQA (VA)	PQMS (VA)	APE (%)
1	24	24	0.000
2	44	44	0.000
3	72	72	0.000
4	107	107	0.000
5	144	144	0.000
6	189	189	0.000
7	243	243	0.000
8	295	295	0.000
9	355	355	0.000
10	417	418	0.178
11	487	487	0.000
12	543	544	0.184
13	595	594	0.168
14	650	651	0.154
15	682	683	0.147
16	458	458	0.000
17	430	430	0.000
18	413	413	0.000
Mean APE			0.046

Table 4.12 presents the apparent power measured from blocked rotor test. The outcomes in 10^{th}, 12^{th}, 13^{th}, 14^{th} and 15^{th} measurement give rise to APE of 0.178%, 0.184%, 0.168%, 0154% and 0.147% respectively, because their PQA and PQMS data is deviated by 1VA. Meanwhile for the verification of system accuracy, a 0.046% mean APE is computed with the inclusion of all the 28 APEs.

Table 4.13: Power Factor Measured from Blocked Rotor Test

Measurement	PQA	PQMS	APE (%)
1	1	1	0
2	1	1	0
3	1	1	0
4	1	1	0
5	1	1	0
6	1	1	0
7	1	1	0
8	1	1	0
9	0.99	0.99	0
10	0.99	0.99	0
11	0.99	0.99	0
12	0.99	0.99	0
13	0.99	0.99	0
14	0.98	0.98	0
15	0.98	0.98	0
16	0.94	0.94	0
17	0.94	0.94	0
18	0.94	0.94	0
Mean APE			0

Out of all the parameters, power factor is the only parameter that achieved mean APE of 0%. It is clearly shown in Table 4.13 that the values recorded by PQA and PQMS are the same for every measurement, thus lead to 0% APE in each measurement.

Table 4.14: Mean APE and Range of APE for Each Parameter

Parameter \ APE	Lowest	Highest	Mean
Voltage	0	0.076	0.036
Current	0	0.311	0.045
Real Power	0	0.283	0.038
Reactive Power	0	0.840	0.047
Apparent Power	0	0.184	0.046
Power Factor	0	0	0

The summarization of the APE range and its mean for the six parameters concerned in Table 4.14 evidently demonstrated that the lowest APE is 0%, but their highest APE are different. In comparisons of all the parameters, reactive power indicated the highest APE (0.840%), followed by current (0.311%), real power (0.283%), apparent power (0.184%), voltage (0.076%) and power factor (0%). To conclude, the mean APE for all parameter is less than 0.05%, implying the similarity of measurements in PQA and PQMS. Hence, the measurements taken by PQMS are considered as accurate.

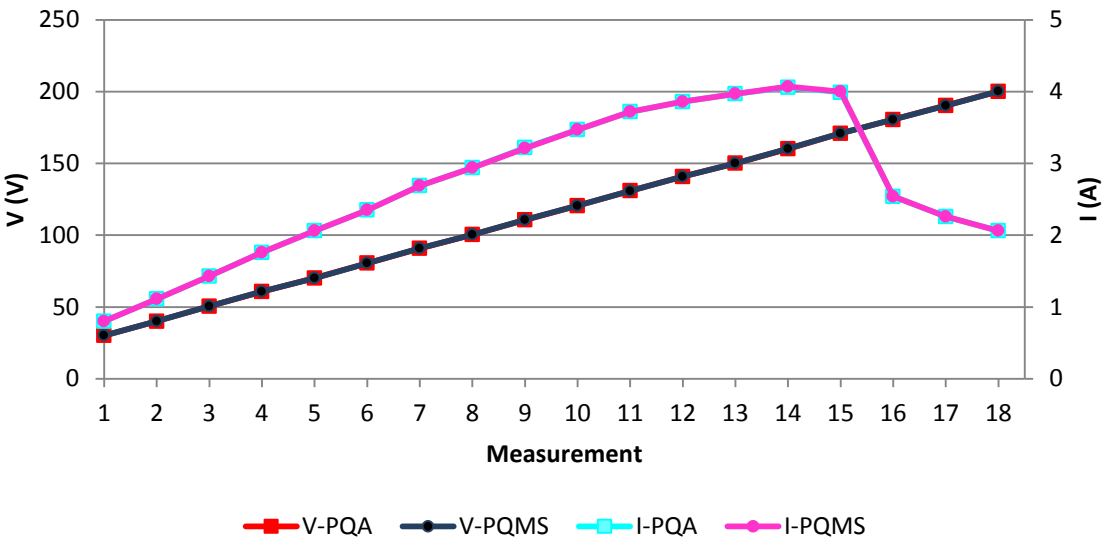

Figure 4.3: Graph of Voltage and Current Measured by PQA and PQMS

In Figure 4.3, the current will appear as approximately 0A for every measurement in case same axes are used. Since the voltage and current recorded by PQA and PQMS are similar, the PQA and PQMS data series tend to overlap each other. The linear increment of PQA and PQMS voltage from 30V to 200V is occasioned from the increment of motor supply by 10V at each measurement. On the other hand, the value of currents went up from 0.8A in 1st measurement to 3.72A in 11th measurement, at a rate of approximately 0.3A for each increment of 10V. They are then increased by about 0.1A at each interval until it reaches 4.06A in 14th measurement for PQA and 4.07A for PQMS, where they experienced a sudden drop to 2.54A in 16th measurement. The currents continued to decline, but not as rapidly as in the 14th to 16th measurements. When the rotor started to move, the current will experienced a sudden drop in its value.

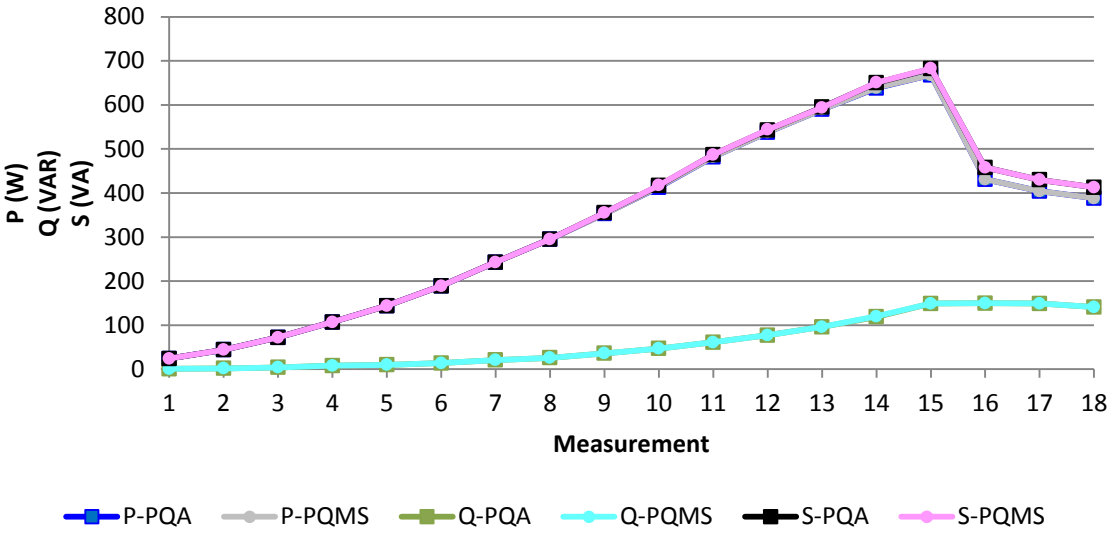

Figure 4.4: Graph of Real Power, Reactive Power and Apparent Power Measured by PQA and PQMS

The graph of real power (P), reactive power (Q) and apparent power (S) measured by PQA and PQMS is disclosed in Figure 4.4. Apparent power rose gradually from 24VA until they hit the peak at 15th measurement with a value of 682VA for PQA and 683VA for PQMS. Then they began to fall drastically to 458VA. After the 16th measurement, apparent power continued to decline at a slower rate. This pattern is also applicable to the real power. The maximum real power of 668W is recorded by PQA and PQMS at the 15th measurement. After that, they experienced a sudden dip to 431W in the next measurement. The gap between real power and apparent power become larger after the 16th measurement, where a difference of 27 existed between the gap. The reactive power exhibited a steady upward trend, which started from 1VAR in the 1st measurement until 149VAR in the 15th measurement. It remained constant for the 16th and 17th measurements, and then it dropped to 141VAR at the 18th measurement.

These changes in real power, reactive power, and apparent power occurred due to the influence of power factor. When the power factor is 0.99 or 1, the values recorded for real power and apparent power are similar. The further decrement in power factor had caused the real power and apparent power to deviate from each other. Likewise, the pattern for reactive power is affected by power factor too. Reactive power increased

gradually when the power factor is above 0.99, whereas it tends to remain constant when the power factor is below 0.99.

4.3 Voltage Sag Performance

Voltage sag signals are generated from three types of load setting, which include six single phase capacitor run motors, four single phase capacitor run motor with RLC load, and a three phase squirrel cage induction motor with transformer. The performance of PQMS in classifying the PQ problem is analyzed with reference to PQA in evaluations of the signals detected by both instruments.

4.3.1 Single Phase Capacitor Run Motor

Two types of single phase motor load are used for generating the sag signals. One consists of six motors while the other is with the combination of four motors and RLC load. These two set ups are chosen for the performance verification of PQMS in PQ problem identification. These arrangements have caused the supply voltage to reduce by at least 10% during the motor startup. After the motor starting, voltage surged to a voltage level lower than the nominal 240V.

Case 1: Motor Only

In Figure 4.5, the starting current for the six capacitor run motors is $28A_{pk}$ which lasted for 1.16 second, has been rapidly deteriorated to $5A_{pk}$. This demonstrates the transition of motor starting current from inrush current to running current.

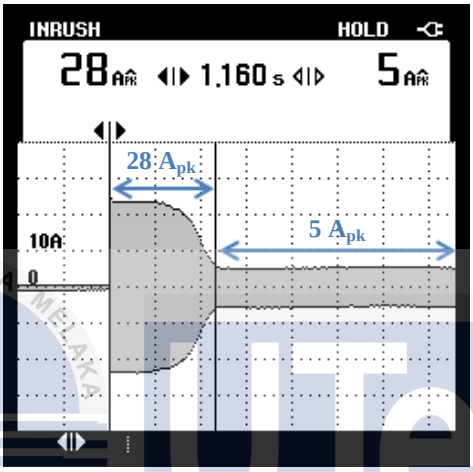

Figure 4.5: Inrush Current by PQA

Before the switch is closed, the supply was initially 240V and 0A because there is no load connected to the supply yet. At the moment of closing the switch, the voltage dropped but the current increased and all of this happened in a very short time. After that, the voltage rose back to a constant voltage of 231.6V, whereas the current remained constant at 4.27A. Voltage and current trend described can be found in Figure 4.6.

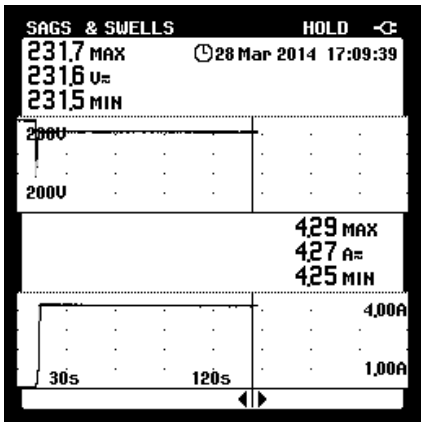

Figure 4.6: Voltage and Current Trend by PQA

Figure 4.7 gives an insight of the waveform results recorded by PQMS. Green line represents the voltage while blue line represents the current. Similar to the trends in Figure 4.6, PQMS recorded an initial voltage of 240V and current of 0A. When the motors are started up at 13th seconds, voltage had suffered a drop and current opposed the voltage. Instead, the current experienced an increment. This situation did not last for long, whereby in the next seconds, the voltage increased to a constant value of 232.47V and the current plummeted to 4.263A. Although there is 3.136% drop in voltage, PQMS classify the signal as "Normal".

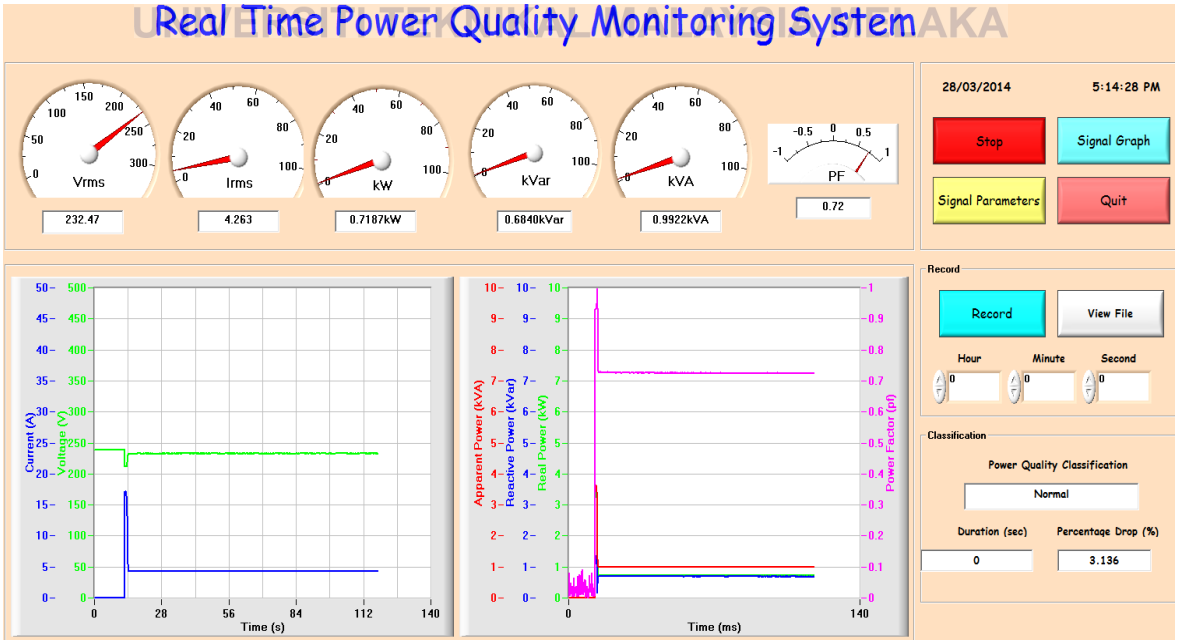

Figure 4.7: PQMS Results

As for the voltage signal in Figure 4.8, the decrement starts from 237.5V to 208.5V before increasing to 231.6V. Thus, the magnitude of sag is 12.21% as calculated from equation 3.3. This satisfied the definition of sag given by IEEE, i.e. the magnitude of sag should be 10% to 90% of the nominal voltage. To be precise, a voltage drop to at least 216V from an initial voltage of 240V is necessary for it to be considered as voltage sag.

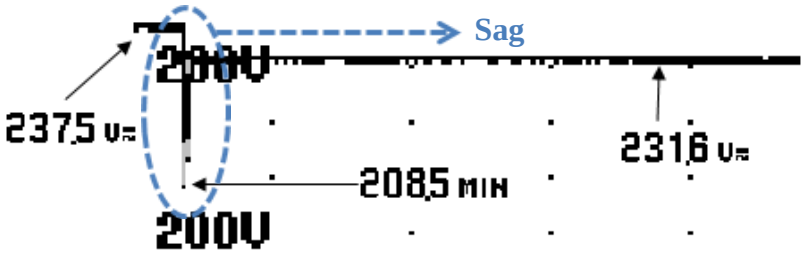

Figure 4.8: Magnified Voltage Waveform by PQA

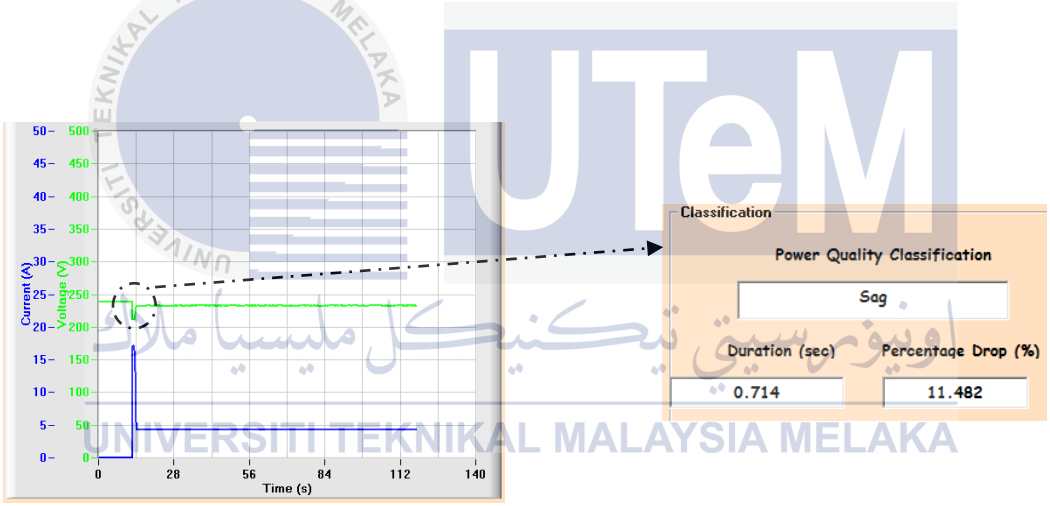

Figure 4.9: Voltage Sag Classification by PQMS

The region which voltage sag happened is indicated in Figure 4.9. It is shown that the sag of 11.482% happened for 0.714 second. During the course of sag event, the voltage measured by PQA decreased to 208.5V from 237.5V, whereas PQMS recorded a decrement of 27.33V from 238V. The percentage of voltage sag in PQMS is lesser than the one calculated for PQA by 0.728%.

Case 2: Motor and RLC Load

Voltage sag signal is obtained successfully by combining the RLC load and capacitor run motors from four stations. In reference to Figure 4.10, when the switch is closed, the motors had drawn starting current of $26A_{pk}$. After 1.28 second later, the starting current had transited to running current of $10A_{pk}$.

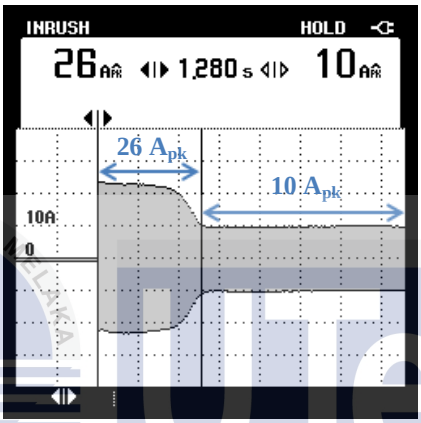

Figure 4.10: Inrush Current for Motor and RLC Load by PQA

Figure 4.11 gives an overview of the voltage and current trends recorded with PQA Sags & Swells function. As usual, the supply experienced a sudden drop in voltage and an increase in current when the motors are switched on. After the motors stabilized, the supply voltage escalated to a value (226.3V) which is lower than nominal voltage (240V). However, the current remained constant at 6.92A following its increment from 0A.

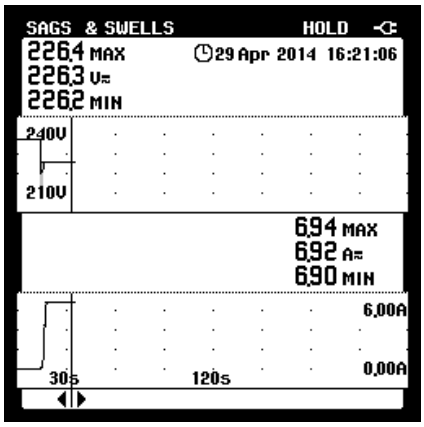

Figure 4.11: Voltage and Current Trend for Motor and RLC Load by PQA

The data recorded with PQMS in Figure 4.12 is similar to that of PQA. Prior to switching on the motors, the voltage remained constant at 237V. Current is 0A because the circuit is incomplete when the switch is opened. Once the switch is closed at the 15th seconds, the voltage dipped and eventually increased to 228.39V. The current has also surged before it declined to 6.334A. As a consequence, PQMS categorized the signal as "Normal" with voltage drop of 4.839% where the percentage represented the deviancy between 228.39V to its nominal voltage 240V.

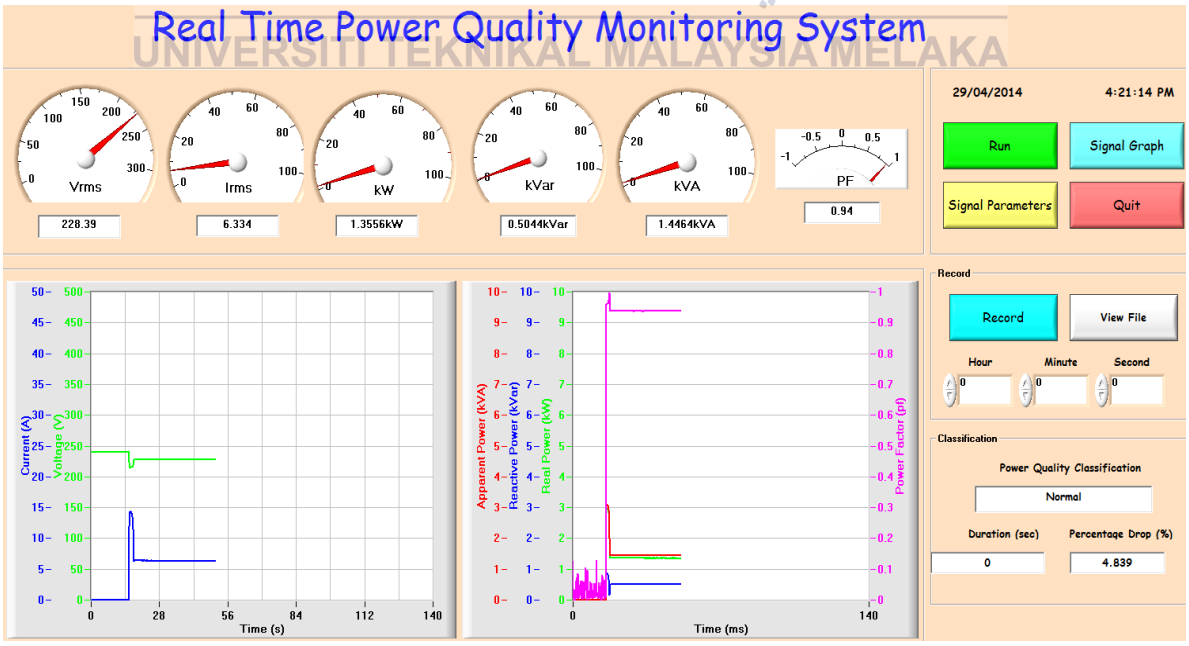

Figure 4.12: PQMS Results

The magnified voltage waveform is shown in Figure 4.13. Following the initiation of motors, the supply voltage of 237.8V fell greatly to 212.7V, but it succeeded in ascending to 226.3V. The calculation from equation 3.3 shows the percentage of sag is 10.56%, proving that the supply is indeed experiencing a voltage sag.

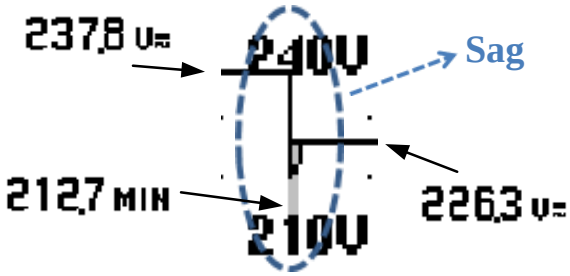

Figure 4.13: Magnified Voltage Waveform by PQA

Figure 4.14 highlights the region where voltage sag had occurred for 0.833 second with 10.484% of voltage drop due to the motor starting. The percentage measured for voltage drop in PQMS is 0.076% lower than percentage calculated for sag in PQA. As the declination of voltage happened in a short time and the signal during sag occurrence is inconstant, the real time signal monitoring has triggered the fluctuation in measurement value.

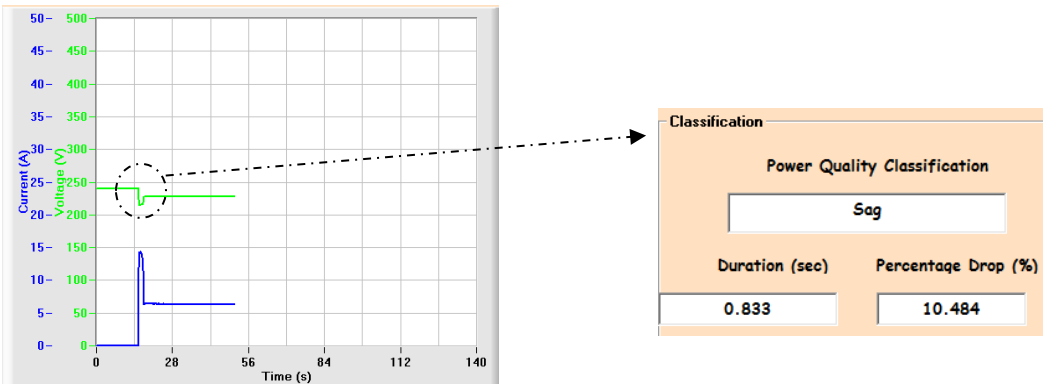

Figure 4.14: Voltage Sag Classification by PQMS

Table 4.15: Voltage Sag Performance for Different Load

Parameter \ Case	1	2
Type of Load	6 capacitor run motors	4 capacitor run motors with RLC load
Starting Current (A_{pk})	28	26
Running Current (A_{pk})	5	10
Supply Voltage (V)	237.5	237.8
Minimum Voltage (V)	208.5	212.7
Percentage of Voltage Drop (%)	12.21	10.56

Comparisons between the results obtained from two different loads are organized in Table 4.15. The results of case 1 and case 2 varied as a result of connecting different loads to the single phase supply. These two cases are chosen for discriminating the effect of loads on the supply voltage drop.

The voltage drop of 6 capacitor run motors is sufficient to be classified as voltage sag, but with the inclusion of RLC load, only 4 motors is required for generating the voltage sag signal. The noticeable difference of starting and running current in both cases is due to the load used. Even though the starting currents are differed by 2A, the running current required in case 2 is twice of that in case 1. The minimum voltages recorded in both cases are 208.5V and 212.7V respectively. Thus, a larger percentage of voltage drop is computed for case 1.

The occurrence of voltage sag in these 2 experiments is an effect from the starting of motor. During the motor starting, it drawn high starting current, which is 6 to 7 times of its rated full load current, resulted a voltage drop in the supply. Due to the small rating of the motor, multiple capacitor run motors are used since the voltage drop in a single motor is not large enough to be classified as voltage sag. Subsequently, high starting current drawn by the 6 single phase motors, as well as the combination of 4 single phase motors and RLC load had induced the voltage sag.

4.3.2 Three Phase Squirrel Cage Induction Motor

Only one three phase motor is required for obtaining the sag signal. A duration of 0.192 second is required for the transition of starting current to running current, as shown in Figure 4.15. The motor starting drew a current of $9.1A_{pk}$. After the motor changed its stage from starting to running, it continued to draw $0.7A_{pk}$.

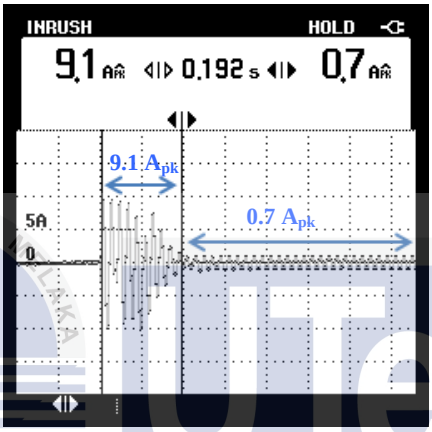

Figure 4.15: Inrush Current by PQA

In Figure 4.16, the initial voltage and current recorded at the supply were 240V and 0A respectively. These values remained constant until the initiation of motor starter. As soon as the motor started to function, the voltage signal experienced a sharp drop in its value and immediately rocketed to 238.5V whereas the current gradually increased to 0.663A. When the motor is still running, the voltage and current remained unchanged, i.e. the values recorded continuously are 238.5V and 0.663A.

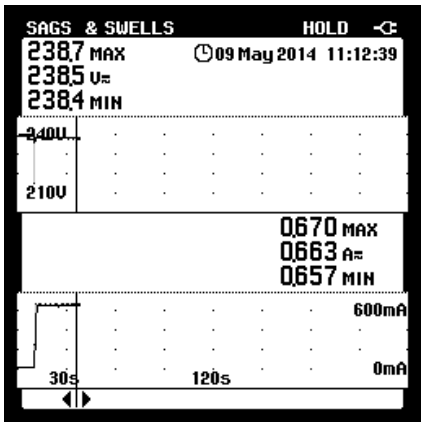

Figure 4.16: Voltage and Current Trend by PQA

Similar to the results recorded by PQA in Figure 4.16, the voltage and current recorded by PQMS in Figure 4.17 exhibited opposing pattern during the starting of motor. The voltage and current measured are 240V and 0A to begin with, but after the motor is started, reduction of voltage and increment of current happened at the same time. This situation does not lasted for long, since the voltage managed to escalate to 237.54V and the current declined to 0.5A. PQMS classified the signal as "Normal" because the signal only experienced a 1.023% drop in voltage at the time of capturing the screenshot.

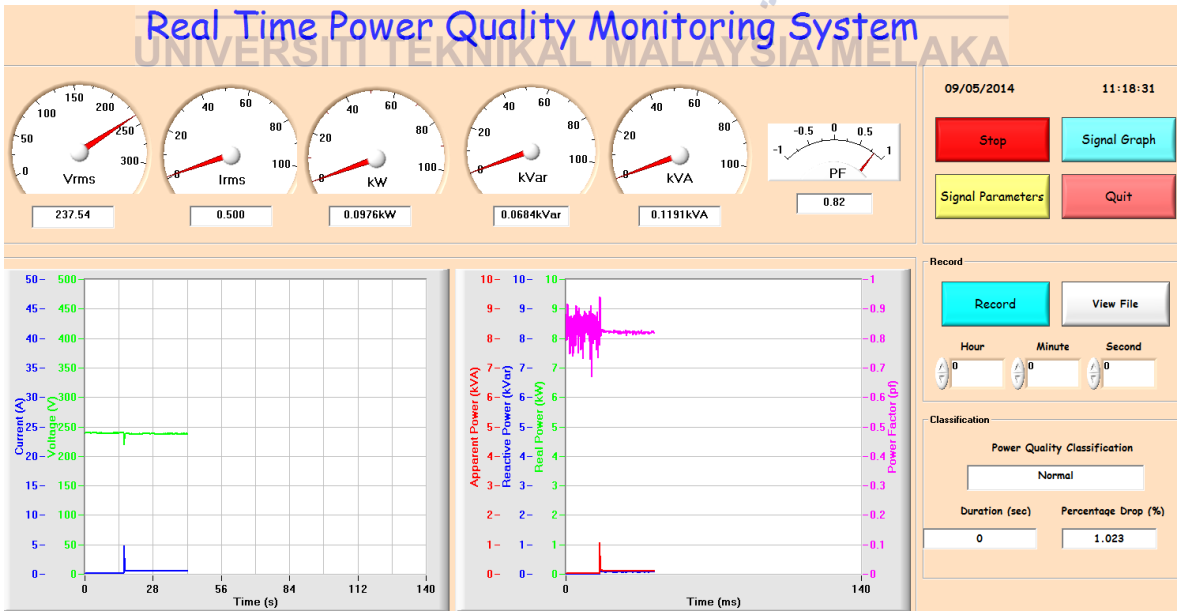

Figure 4.17: PQMS Results

The magnified voltage trend of Figure 4.16 is given in Figure 4.18. First, 240V is measured prior to the motor starting. It is then sag to 215.8V during motor starting, where the minimum voltage recorded at this point is considered. The resulted percentage of voltage drop due to motor starting is 10.08%, which satisfied the requirement of IEEE for a signal to be classified as sag. After dropping to 215.8V, the voltage instantaneously stabilized to 238.5V.

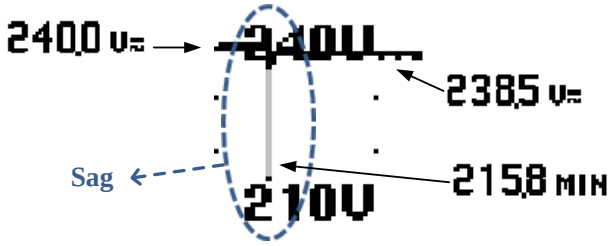

Figure 4.18: Magnified Voltage Trend by PQA

Significantly, a voltage drop of at least 10% can be classified as sag. Voltage sag with a drop of 10.035% for 0.322 second has occurred in the region marked in Figure 4.19. PQA presents a voltage drop which is 0.045% higher than PQMS. Before the sag event, both recorded an initial voltage of 240V. Once the switch is initiated, PQA measured 215.8V whereas PQMS measured 215.92V. These deviations in measurement have led to the different percentage of voltage drop. Since the percentage is within 0.05%, the efficiency of the system is proven in conjunction with PQA.

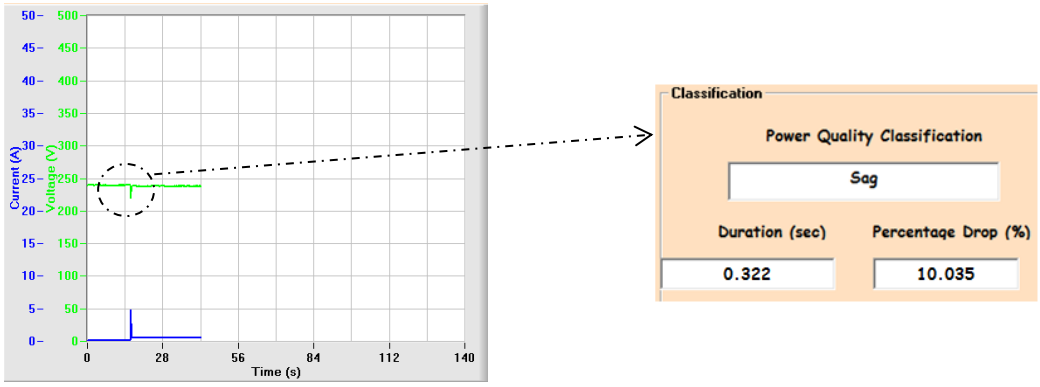

Figure 4.19: Classification of Voltage Sag in PQMS

4.4 Harmonic Distortion

Harmonic distortion signals are investigated through single phase full wave controlled rectifier and three phase motor. Similar to voltage sag performance analysis, the comparisons of results obtained by PQA and PQMS has proven the effectiveness of PQMS in identifying power quality disturbances.

4.4.1 Single Phase Full Wave Controlled Rectifier

Three cases are being considered in this experiment. Case 1 and case 2 are to determine the amount of RLC load that will results in the disturbance which qualified to be classified as harmonics. Two different firing angles are chosen, i.e. 100.5° for case 1 and 50.6° for case 2. Lastly, the purpose of the third case is to examine the effect of firing angle increment while maintaining the load. The load obtained in case 2 remained constant whilst the firing angle is increased from 50.6° to 100.5°. Analysis of voltage and current signals is made by comparing the amplitude and pattern of waveshapes obtained through PQA and PQMS. The PQA and PQMS spectrum results are also compared in terms of pattern similarity against the frequency.

Case 1: Firing Angle = 100.5°, R = 4800 Ω, L = 3.8H or 1200Ω, C = 1.33μF or 2400Ω

For firing angle of 100.5°, it is found that RLC load valued as R = 4800 Ω, L = 3.8H or 1200Ω, C = 1.33μF or 2400Ω has produced the disturbance that can be classified as harmonic, as presented in Figure 4.20. Figure 4.21 shows that the disturbance has

occurred for 128.570s while the percentage of voltage drop is 2.669%. The presence of voltage drop percentage is due to the voltage measured is lower than 240V.

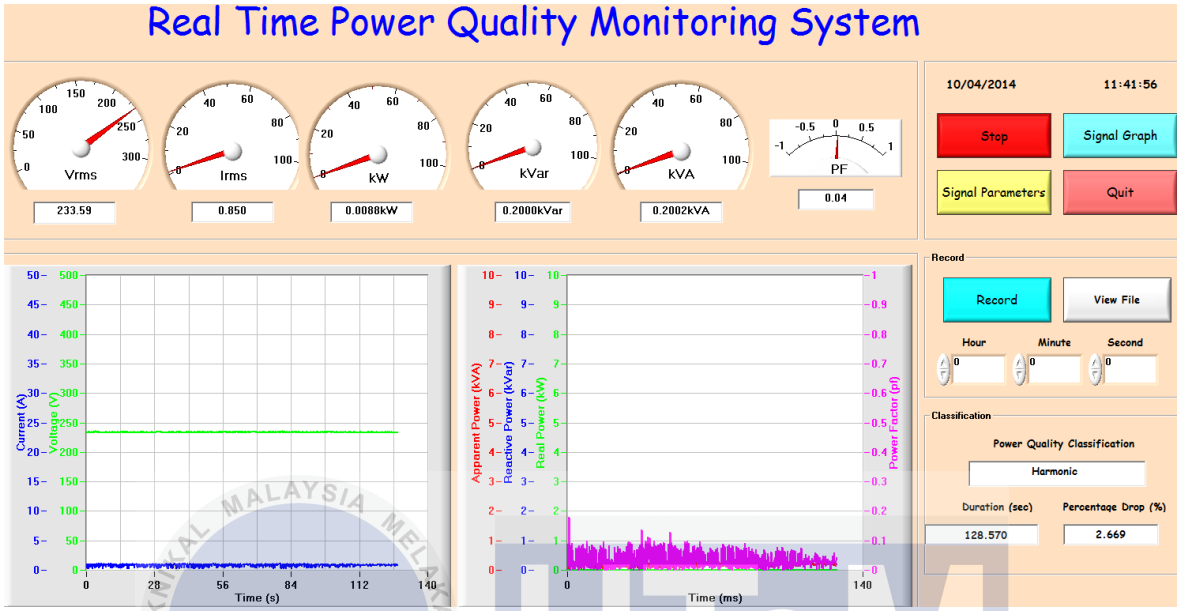

Figure 4.20: PQMS Results for Case 1

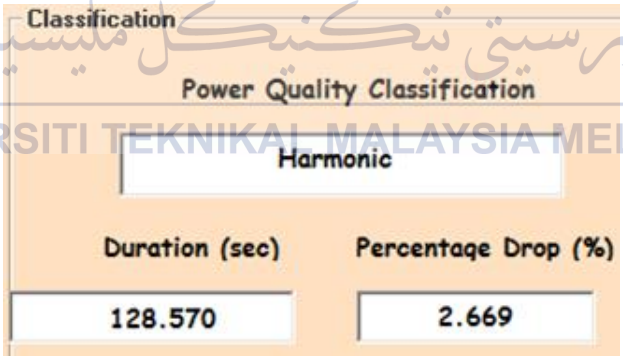

Figure 4.21: PQMS Classification Result for Case 1

Figure 4.22(a) shows that the combination of such RLC load has resulted in 242.6V and 0.93A. This satisfied the requirements of voltage to be more than 216V and current to be lower than 1A. Both the waveforms displayed in PQA and PQMS resembled each other. It can be seen that the upper limit of the distorted voltage signal is about 450V while the lower limit is about 250V. As for the current signal, PQMS in Figure 4.22(b) shows that

there are sudden spike ranged from 10A to 14A, but the PQA only shows the spike at value 14A. The waveforms and the value measured for voltage and current can be found in Figure 4.22(a) and (b). These waveforms are not of perfect sinusoidal wave shape due to the presence of harmonic components in the waveforms.

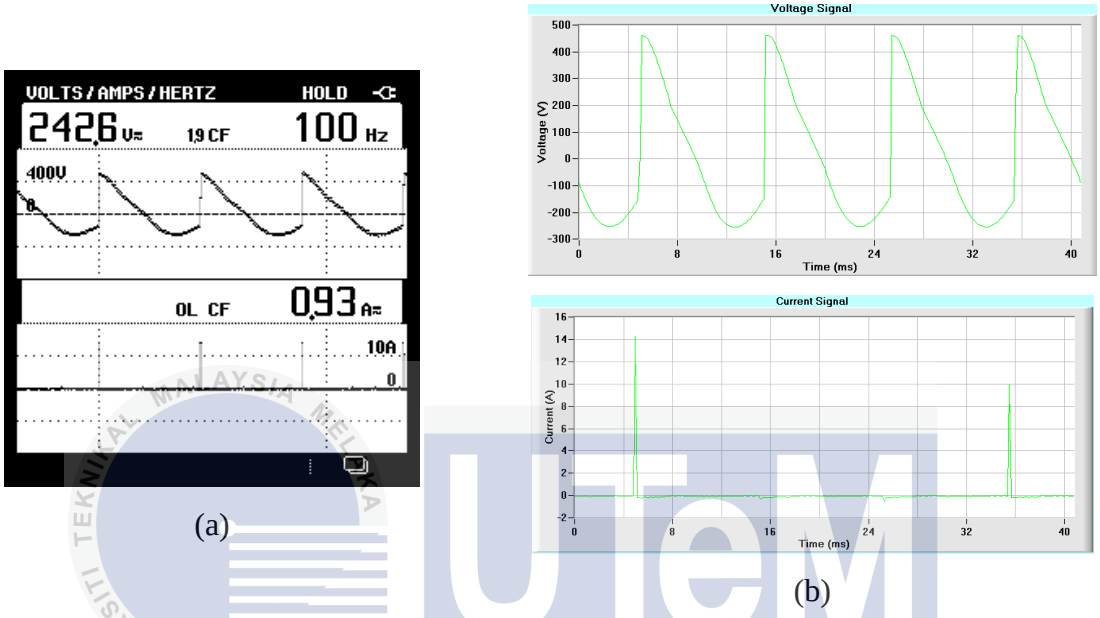

(a) (b)

Figure 4.22: Voltage and Current Waveforms as Recorded by (a) PQA (b) PQMS

Figure 4.23(a) depicts the voltage harmonic spectrum recorded by PQA whereas Figure 4.23(b) shows the voltage power spectrum recorded by PQMS. The spectrum trend is similar for both instruments, where the magnitude at 100Hz is the highest then it fall sharply at 200Hz. After that, it exhibits a steady declining trend.

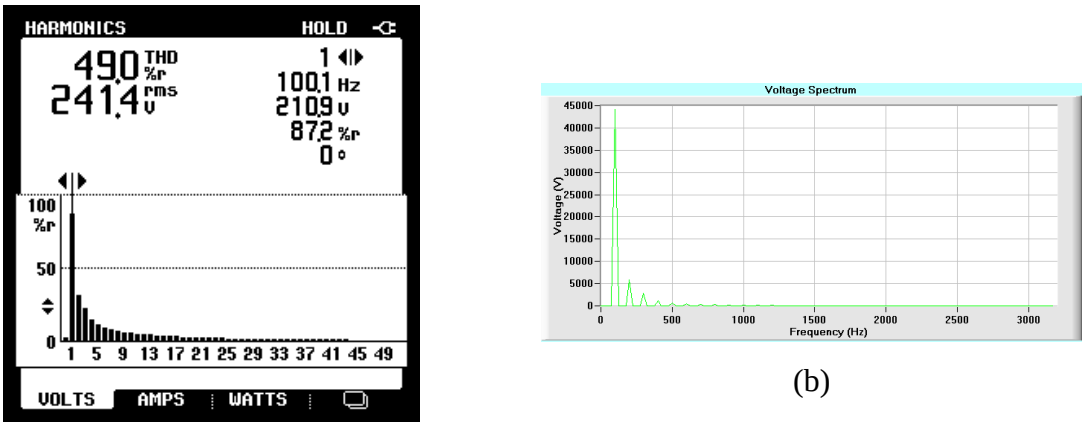

(a) (b)

Figure 4.23: Voltage Spectrums as Recorded by (a) PQA (b) PQMS

Aside from spectrums for voltage signal, PQA and PQMS have also recorded the spectrums for current signal. The magnitude increased gradually until 300Hz, and then it fluctuated in a wave-like trend as shown in Figure 4.24(a). Similar frequency wave trend can also be observed in current power spectrum of Figure 4.24(b).

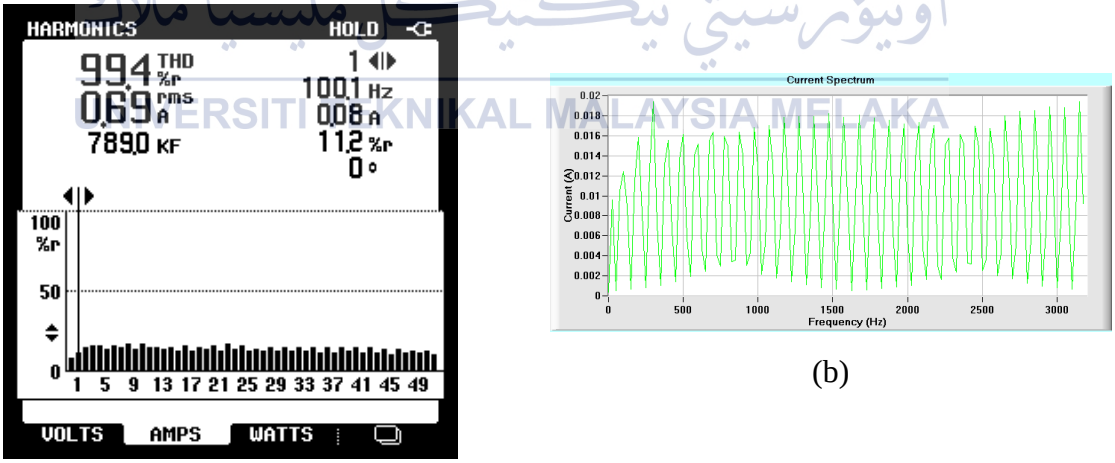

(a) (b)

Figure 4.24: Current Spectrums as Recorded by (a) PQA (b) PQMS

Decrement of firing angle while maintaining the load, resulted in the increment of voltage and current. Since the rating of thyristor is 1A, the increment in current lead to the tripping of system. Conversely, the voltage and current reduces as a result of firing angle increment.

Case 2: Firing Angle = 50.6°, R = 686Ω, L = 15.3H or 4800Ω, C = 0.66μF or 4800Ω

At lower firing angle, in this case 50.6°, the disturbance that is resulted from the RLC load, where R = 686Ω, L = 15.3H or 4800Ω, C = 0.66μF or 4800Ω, is categorized as harmonic. Figure 4.25 implies that the harmonics has occurred for 60.667s and the voltage recorded is lower than its nominal 240V by 3.940%. The classification result is shown in Figure 4.26.

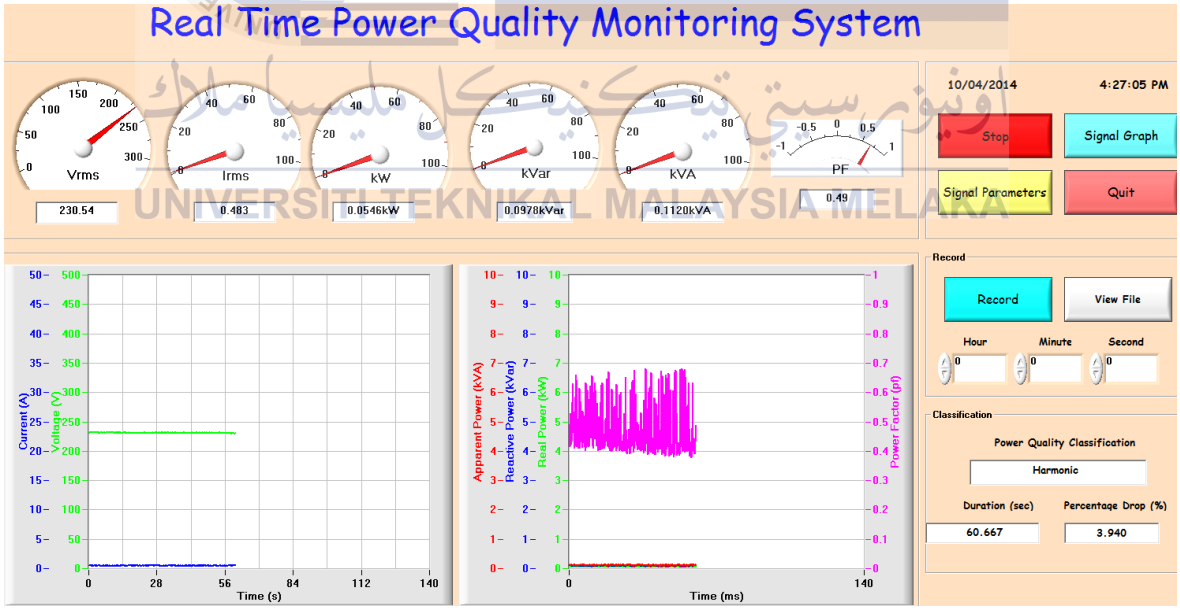

Figure 4.25: PQMS Results for Case 2

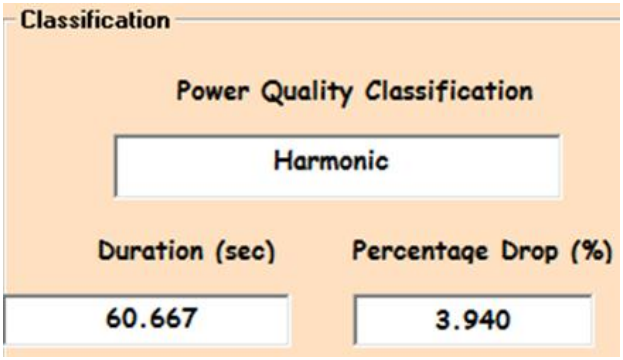

Figure 4.26: PQMS Classification Result for Case 2

The reading of 231.7V and 0.509A are recorded as soon as the RLC load is connected to the system. In Figure 4.27, the voltage and current signals are similar in both PQA and PQMS. The trapezoidal-shaped voltage signals shown by PQA and PQMS exhibit an upper limit of 320V and lower limit of -110V. Meanwhile, both the current signals appeared as a combination of impulse and low magnitude sine wave. The current impulses with amplitude 5A or 6A as given in Figure 4.27(b) occurred at interval of 1 cycle, as shown in Figure 4.27(a). The waveforms are distorted due to the presence of harmonic components in voltage and current signals.

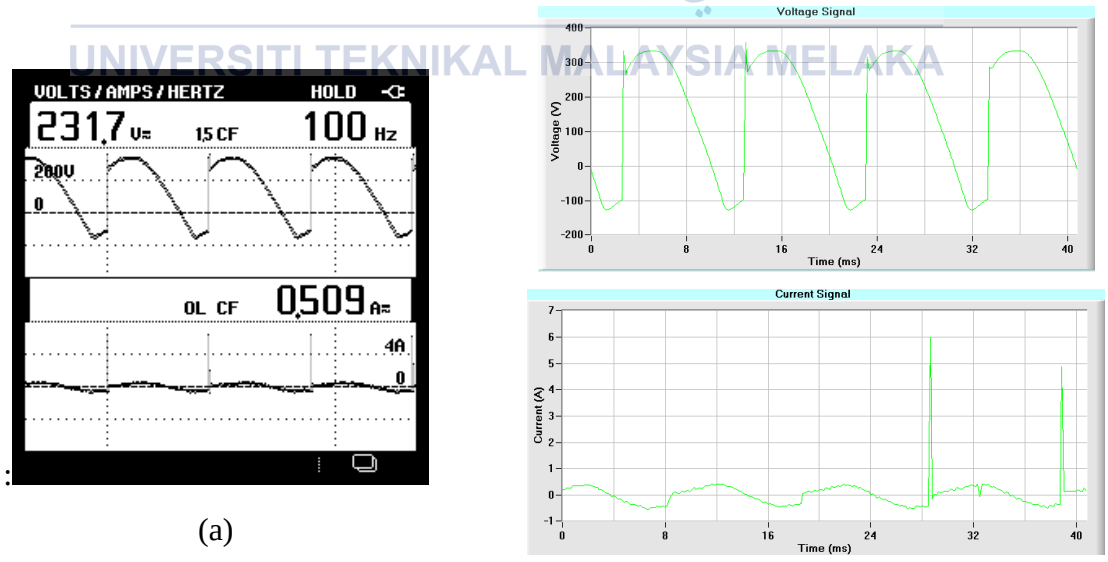

(a)

(b)

Figure 4.27: Voltage and Current Waveforms as Recorded by (a) PQA (b) PQMS

The voltage spectrums in Figure 4.28(a) increased slightly from 0Hz to 100Hz. It is then declined rapidly at 200Hz and from there onwards, it continued to decline gradually. Similar pattern of frequency is observed from the voltage power spectrum recorded by PQMS in Figure 4.28(b), where the values at 0Hz and 100Hz are much greater than the other frequencies.

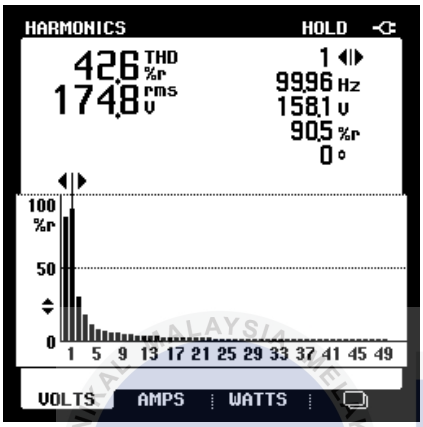

(a)

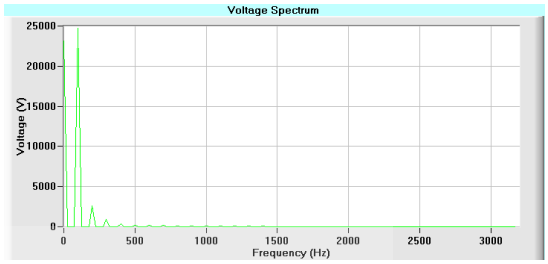

(b)

Figure 4.28: Voltage Spectrums as Recorded by (a) PQA (b) PQMS

The current spectrums for case 2 are presented in Figure 4.29(a). Generally, the magnitude at 100Hz is the highest among all the other magnitudes. The constant magnitude at 200Hz and 300Hz dropped slightly at 400Hz, then they remained constant with no fluctuation pattern. As for the current power spectrum in Figure 4.29(b), only first to third orders are visible, whereby the fundamental is the highest.

(a)

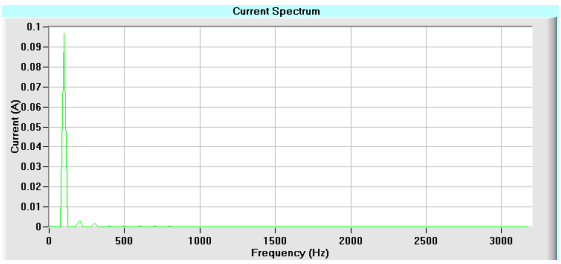

(b)

Figure 4.29: Current Spectrums as Recorded by (a) PQA (b) PQMS

At low firing angle, the current can surge to more than 1A with load variation and this will trip the system. When the firing angle is increased without regulating the load, both voltage and current will experience a decrement.

Case 3: Firing Angle = 50.6° → 100.5°, R = 686Ω, L = 15.3H or 4800Ω, C = 0.66μF or 4800Ω

When firing angle is increased from 50.6° to 100.5° whilst maintaining the load, for instance R = 686Ω, L = 15.3H or 4800Ω, C = 0.66μF or 4800Ω, it is noticed that the voltage and current had decreased significantly in Figure 4.30. The voltage and current dropped along with the increment in firing angle. Thus, the decrease in voltage to a value less than 216V has led the PQMS to classify the disturbance as sag. Figure 4.31 indicates that sag had occurred for 28.810s and the voltage is lower than its nominal value by 32.983%.

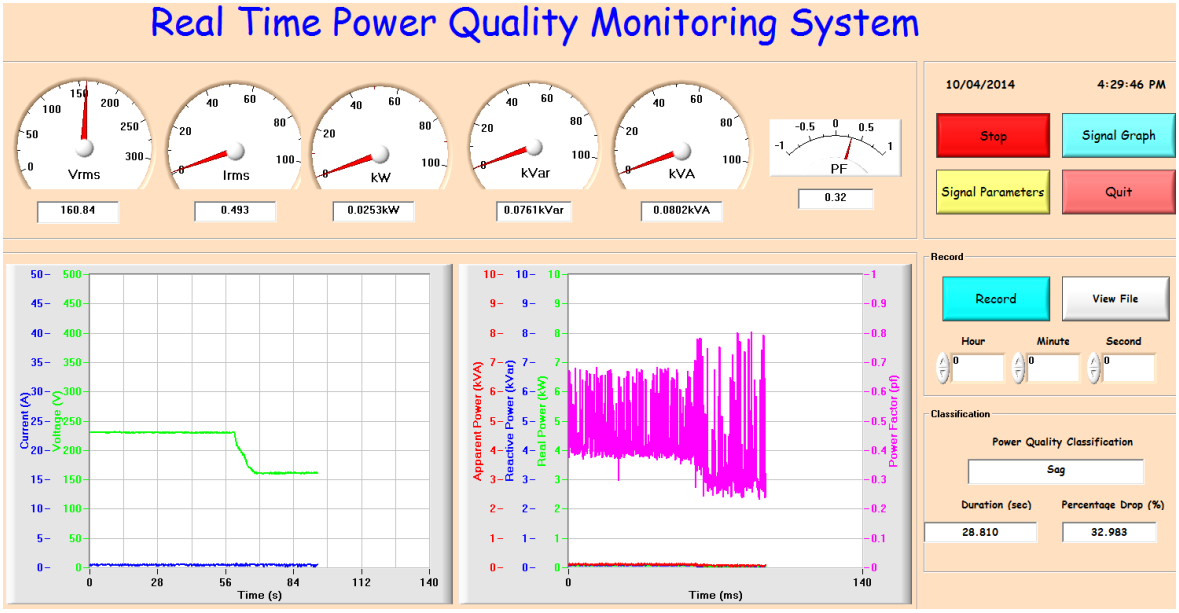

Figure 4.30: PQMS Results for Case 3

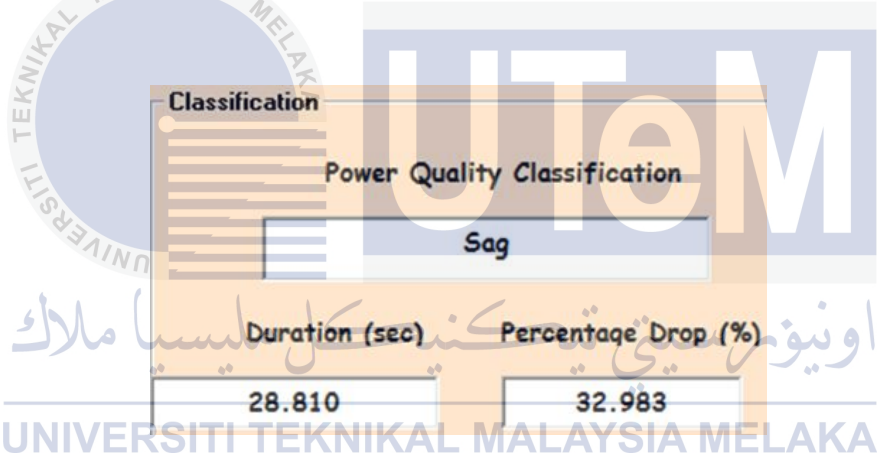

Figure 4.31: PQMS Classification Result for Case 3

The value of voltage and current measured as shown in Figure 4.32(a) are 161.2V and 0.427A respectively. From Figure 4.32(a) and (b), saw tooth-like waveform with amplitude range of -90V and 450V is observed for the voltage signal whereas the current signal is shown as sudden spikes with amplitude of 8A at each cycle of wave. It is noted that the voltage waveform has changed from trapezoidal shape in Figure 4.27 into saw tooth shape with amplitudes in the range of -100V to 320V, but only slight changes occurred in current waveform.

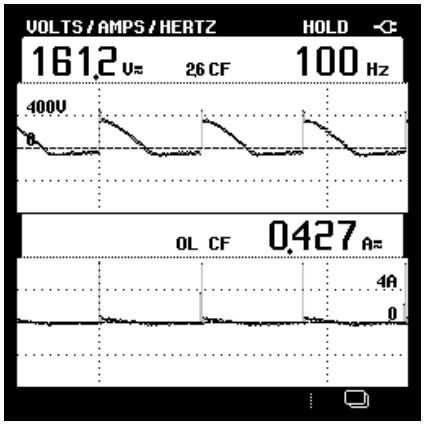

(a)

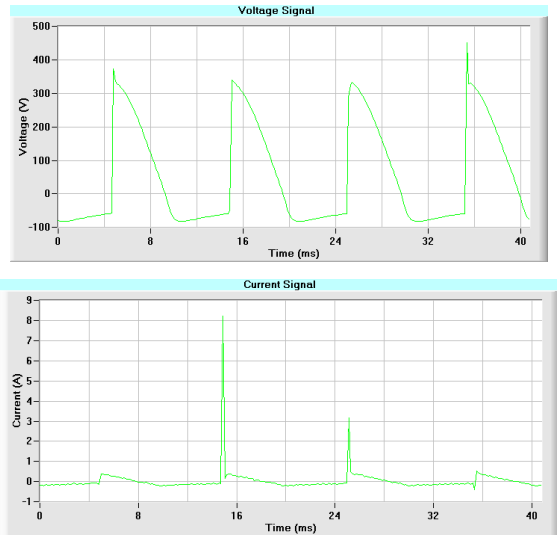

(b)

Figure 4.32: Voltage and Current Waveforms as Recorded by (a) PQA (b) PQMS

The spectrums in Figure 4.33(a) and (b) show great resemblance in term of their magnitude variation pattern. The highest magnitude occurred at 100Hz, followed by 0Hz and 200Hz. Then, the magnitude, starting from 300Hz, decreased steadily. There is not much difference in the voltage spectrum between case 2 and case 3, except for the dc component of case 3 in Figure 4.33(a) has reduced by half of its height compared to Figure 4.28(a) in case 2. Fundamental component remained to be the highest. As the order increases, the magnitude becomes lower. Similarly, the voltage power spectrum has also been affected. The spectrum in Figure 4.33(b) suffered a 25% reduction compared to Figure 4.28(b).

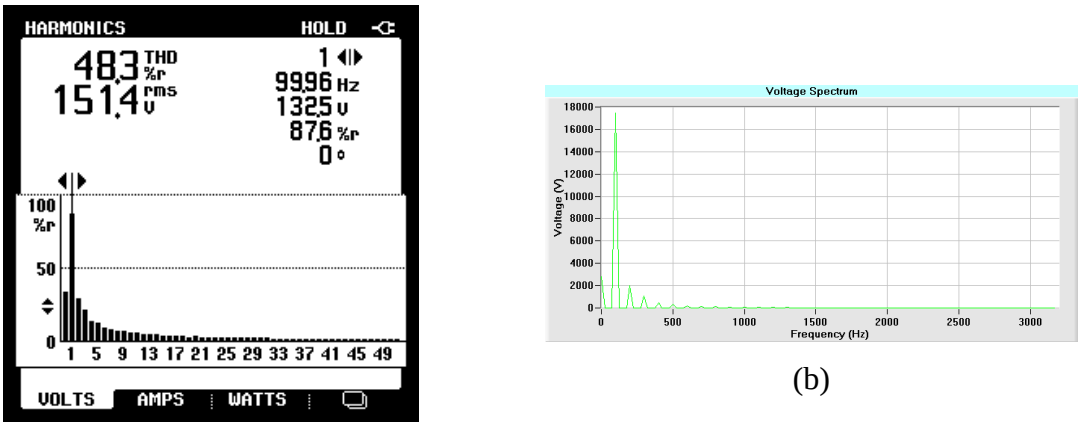

(a) (b)

Figure 4.33: Voltage Spectrums as Recorded by (a) PQA (b) PQMS

After the decreasing pattern that occurred at 200Hz and 300Hz, the spectrums in Figure 4.34(a) and (b) have remained constant. The lowest and highest magnitude of the spectrums is found at 0Hz and 100Hz respectively. A clear distinction between the current power spectrum recorded by PQMS in both case 2 and case 3 is that all the spectrums can be seen clearly in Figure 4.34(b), whereas only first order is visible in Figure 4.29(b). The spectrum trends in Figure 4.34(a) bear great resemblance to the one in Figure 4.29(a). Contrarily, the magnitudes from 200Hz onwards are slightly higher than the one in case 2. The fundamental is a special case, instead of becoming higher, it is reduced by one-third of its height.

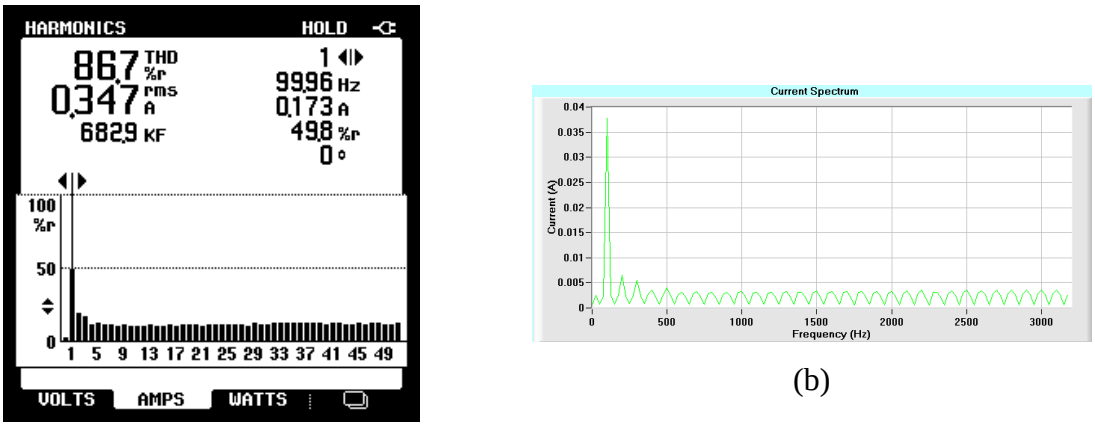

(a) (b)

Figure 4.34: Current Spectrums as Recorded by (a) PQA (b) PQMS

Table 4.16: Effect of Firing Angle and Load on the Voltage, Current and Their THD

Parameter / Case	Firing Angle (°)	Load (Ω)	Voltage (V)	Current (A)	THD_V (%)	THD_I (%)
1	100.5	R = 4800 L = 1200 C = 2400	242.6	0.93	49.0	99.4
2	50.6	R = 686 L = 4800 C = 4800	231.7	0.509	42.6	64.9
3	50.6→100.5	R = 686 L = 4800 C = 4800	161.2	0.427	48.3	86.7

The summary in Table 4.16 infers that, different RLC load is needed at various firing angle in order to raise the voltage to more than 216V. For instance, when the firing angle is 100.5°, a RLC load of R = 4800Ω, L = 1200Ω and C = 2400Ω will produce 242.6V. Alternatively, an output of 231.7V is produced when RLC load with R = 686Ω, L = 4800Ω and C = 4800Ω is connected to the circuit at firing angle of 50.6°. An increment of firing angle from 50.6° to 100.5° at a load of R = 686Ω, L = 4800Ω and C = 4800Ω caused the voltage to suffer a severe drop from 231.7V to 161.2V.

The amount of current flowing in the circuit is dependent on the load inserted to the circuit. Obviously, in case 2 and case 3 with the same firing angle 100.5°, the current flowing in the circuit varies due to the difference in load. The load currents of 0.93A and 0.427A are measured in case 1 and case 3 respectively. Specifically, current is higher at a lower firing angle in the condition of constant load. This is perceptible in case 2 and case 3, where 0.509A and 0.427A are measured at 50.6° and 100.5°, thus an addition in angle by 49.9° made the current to decrease by 0.082A.

At higher firing angle, the THD tends to increase, especially for THD_I. Even with different load, both THD_V and THD_I at higher firing angle are higher than the one at lower firing angle. It can be seen clearly that THD_V for case 1 and case 3, 49.0% and 48.3%

respectively, are higher than the one in case 2, 42.6%. Similarly for THD_I, 99.4% in case 1 and 86.7% in case 3 are generally much higher than 64.9% in case 2. In the case where firing angle is 100.5°, the one with larger load will generate higher THD, as observed in case 1 and case 3.

4.4.2 Three Phase Squirrel Cage Induction Motor

The voltage and current output waveforms are presented in Figure 4.35(a) and (b). PQA and PQMS have recorded similar wave shapes for both voltage and current. The peak values of PQMS voltage waveforms are -340V and 340V, whereas for current waveforms are -0.7A and 0.8A. Similar value is recorded for PQA voltage waveform, the peak values of current are -0.8A and 0.8A respectively.

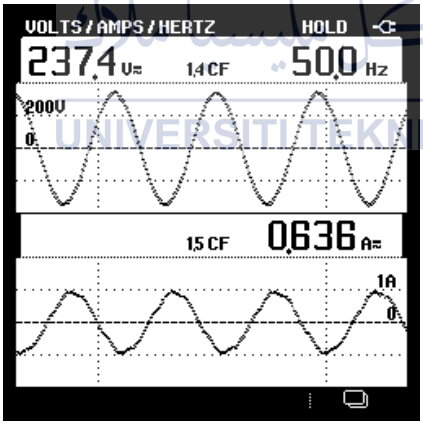

(a)

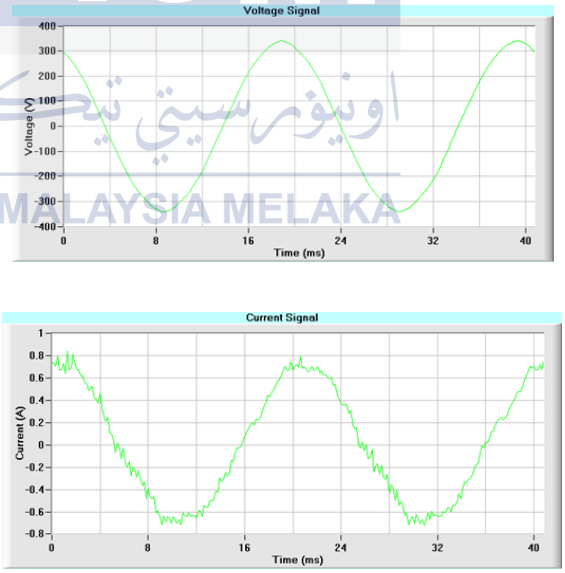

(b)

Figure 4.35: Voltage and Current Waveforms as Recorded by (a) PQA (b) PQMS

Only first order of voltage harmonic spectrum and voltage power spectrum are present in Figure 4.36(a) and (b) correspondingly. PQA indicates that 1.0% of THD_V occurred in the supply. Instead of numbers, the THD_V measured by PQMS is represented in a green line graph. Before switching on the motor, THD_V tends to fluctuate from 0.9% to 1.25%. In fact, the spikes that crossed over the green line indicate the starting time for the motor to be functionalized. Even when the motor functions, the THD_V was still fluctuated within the range of 0.85% to 1.2%.

Only first order of voltage harmonic spectrum and voltage power spectrum are presented in Figure 4.36(a) and (b) correspondingly. PQA indicates that 1.0% of THD_V occurred in the supply. Instead of numbers, the THD_V measured by PQMS is represented in a green line graph. Before switching on the motor, THD_V tends to fluctuate from 0.85% to 1.3%. In fact, the spikes that crossed over the green line indicate the starting time for the motor to be functionalized. Even when the motor functions, the THD_V was still fluctuated within the range of 0.85% to 1.22%.

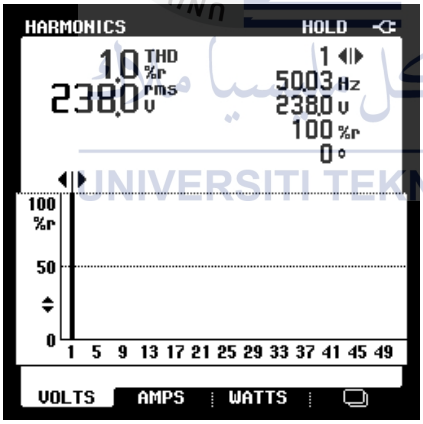

(a)

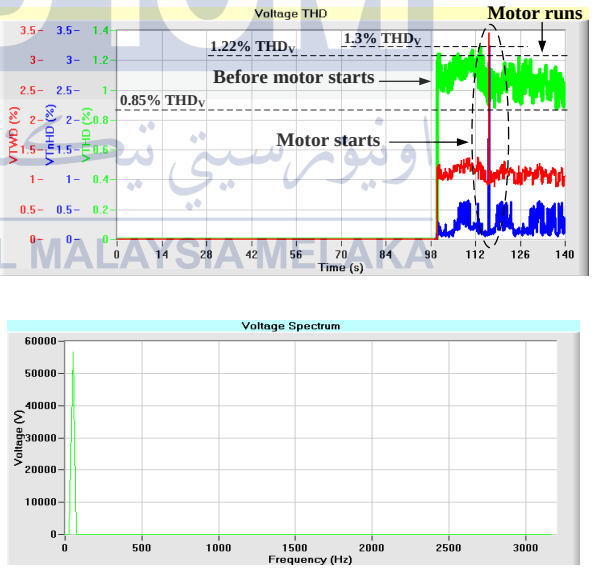

(b)

Figure 4.36: Voltage Spectrums and THD_V as Recorded by (a) PQA (b) PQMS

First harmonic is the highest compared to the rest of the harmonic components. Current harmonic spectrum in Figure 4.37(a) is distinguishable from current power spectrum in Figure 4.37(b). As observed in Figure 4.37(b), PQMS had initially plotted the THD_I once the supply is turned on. Therefore, the green line that fluctuated from 18% to 48% represents the THD_I occurring before motor initiation. It is then declined steeply to 5% and barely visualized due to the lines overlapping on top of the green line. Likewise, the PQA THD_I measurement of 5.2% deviates by 0.2% from the THD_I measured by PQMS.

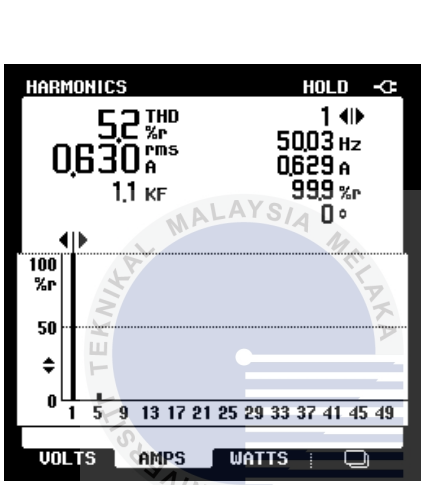

(a)

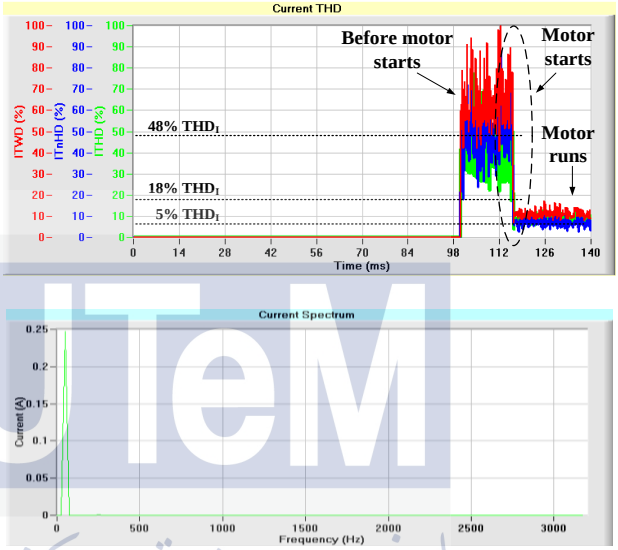

(b)

Figure 4.37: Current Spectrums and THD_I as Recorded by (a) PQA (b) PQMS

CHAPTER 5

CONCLUSION AND RECOMMENDATION

5.1 Conclusion

This project was set out to justify the performance of PQMS in reference to Fluke 43B PQA. The PQMS proposed is capable in measuring and monitoring the power system in real time. Different types of experiment set ups have contributed valuable data for analysing the performance of PQMS. Utilization of those experiments also assisted the PQMS capability test in measurement and PQ event classification. The PQMS accuracy in measurements is proven through no load test and blocked rotor test. Likewise PQMS succeeded in identifying PQ problems such as voltage sag and harmonic distortion created from single phase and three phase laboratory set ups. Comparisons in terms of percentage of voltage sag during motor starting and spectrums against frequency for harmonics showed the similarity between the PQA and PQMS results.

The APE from each measurement is used for evaluating the PQMS accuracy in measuring power system parameters. APE shows the percentage of deviation between the results recorded by PQA and PQMS. A low APE means that the difference in value is small. Typically, a system with APE lower than 0.05% is regarded as efficient. The signals captured on both instruments during each PQ event show great resemblance, thus assessments of the signals had indicated the feasibility of PQMS in PQ problem classification.

5.2 Recommendation

There are still many types of PQ problems yet to be investigated on PQMS. Some of the PQ events recommended for future work are voltage swell, transients, undervoltage and overvoltage. Improvement to the test results obtained in this project can also be considered. For example, alternative methods for obtaining voltage sag. In this project, the sag is logged during the motor starting and the duration of this sag is very short. Alternative approaches that can cause a longer duration voltage sag during the operation of an equipment should be brainstormed. Instead of the voltage sag due to motor starting, perhaps voltage variation due to large load adding or shedding can be considered.

REFERENCES

[1] S. H. Mohibullah, Laskar, "Power Quality Issues and Need of Intelligent PQ Monitoring in the Smart Grid Environment," *Universities Power Engineering Conference (UPEC), 2012 47th International*, pp. 1–6, 2012.

[2] A. Karaarslan and I. Iskender, "Analysis and Comparison of Current Control Methods on Bridgeless Converter to Improve Power Quality," *International Journal of Electrical Power & Energy Systems*, vol. 51, pp. 1–13, Oct. 2013.

[3] A. R. Abdullah, N. A. Abidullah, N. H. Shamsudin, N. H. H. Ahmad, and M. H. Jopri, "Power Quality Signals Classification System using Time-frequency Distribution," *Applied Mechanics and Materials*, vol. 494–495, pp. 1889–1894, 2014.

[4] P. Y. Yin, M. V Chilukuri, and S. Member, "Remote Power Quality Monitoring and Analysis System Using LabVIEW Software," no. May, pp. 5–7, 2009.

[5] IEEE, *IEEE Std 1159™-2009, IEEE Recommended Practice for Monitoring Electric Power Quality*, vol. 2009, no. June. 2009.

[6] H. W. Beaty and D. Fink, *Standard Handbook for Electrical Engineers*, 16th ed. McGraw-Hill Professional, 2012.

[7] M. H. J. Bollen and I. Y. H. Gu, "Introduction," in *Signal Processing of Power Quality Disturbances*, U.S.A, 2006, pp. 4–15.

[8] R. Baxter, "Storage and The Electric Power Industry," in *Energy Storage: A Nontechnical Guide*, PennWell Books, 2005, pp. 20–21.

[9] P. Caramia, G. Carpinelli, and P. Verde, *Power Quality Indices in Liberalized Markets*. John Wiley & Sons, Ltd, 2009.

[10] M. A. Golkar, "Electric Power Quality : Types and Measurements," *Electric Utility Deregulation, Restructuring and Power Technologies, 2004. (DRPT 2004). Proceedings of the 2004 IEEE International Conference on*, vol. 1, pp. 317–321, 2004.

[11] J. B. Dixit and A. Yadav, *Electrical Power Quality*. Laxmi Publications, Ltd., 2010.

[12] P. Gill, "Power Quality, Harmonics, and Predictive Maintenance," in *Electrical Power Equipment Maintenance and Testing*, 2nd ed., FL: CRC Press, 2009, pp. 719–720.

[13] J. A. Oliver, R. Lawrence, and B. B. Banerjee, "How to Specify Power Quality Tolerant Process Equipment," *Petroleum and Chemical Industry Conference, 2000. Record of Conference Papers. Industry Applications Society 47th Annual*, pp. 281–289, 2000.

[14] A. D. Femine, D. Gallo, C. Landi, and M. Luiso, "Performance Analysis of Power Quality Monitoring Instruments," *Instrumentation and Measurement Technology Conference Proceedings, 2008. IMTC 2008. IEEE*, pp. 2026–2031, 2008.

[15] C. Chen, "Virtual Multifunction Power Quality Analyzer Based on Adaptive Linear Neural Network," *Industrial Electronics, IEEE Transactions on*, vol. 59, no. 8, pp. 3321–3329, Aug. 2012.

[16] A. E. Legarreta, J. A. Bortolin, and J. H. Figueroa, "An IEC 61000-4-30 Class A — Power Quality Monitor: Development and Performance Analysis," *Electrical Power Quality and Utilisation (EPQU), 2011 11th International Conference*, pp. 1–6, 2011.

[17] M. De Apráiz, J. Barros, and R. I. Diego, "Detection and Analysis of Transient Disturbances in A Low Voltage Supply System," *Applied Measurements for Power Systems (AMPS), 2013 IEEE International Workshop*, pp. 35–39, 2013.

[18] D. Gallo, C. Landi, and N. Rignano, "Real-Time Digital Multifunction Instrument for Power Quality Integrated Indexes Measurement," *Instrumentation and Measurement Technology Conference, 2006. IMTC 2006. Proceedings of the IEEE*, no. April, pp. 2271–2276, 2006.

[19] J. Jos é, G. De, J. M. S. Fern ández, and A. Ag üera-pérez, "HOS-based Virtual Instrument for Power Quality Assessment," no. 2, pp. 1–5, 2011.

[20] D. Pradhan, L. Lakshminarayanan, and V. Patil, "A LabVIEW Based Power Analyzer," *Advances in Energy Conversion Technologies (ICAECT), 2014 International Conference on*, pp. 67–71, 2014.

[21] C. Chompoo-Inwai and J. Mungkornassawakul, "A Smart Recording Power Analyzer Prototype Using LabVIEW and Low-Cost Data Acquisition (DAQ) in Being a Smart Renewable Monitoring System," *2013 IEEE Green Technologies Conference (GreenTech)*, pp. 49–56, Apr. 2013.

[22] J. Barros, M. de Apraiz, and R. I. Diego, "A Virtual Measurement Instrument for Electrical Power Quality Analysis using Wavelets," *Measurement*, vol. 42, no. 2, pp. 298–307, Feb. 2009.

[23] R. Jabbar, M. Al-Dabbagh, M. Akmal, and K. Latif, "A Practical Technique for Power Quality Improvement for Single Phase Induction Machines," 2006.

[24] V. G. Neve, G. M. Bonde, and G. M. Dhole, "A Comparative Study for Detection and Measurement of Voltage Disturbance in Online Condition."

[25] A. P. Memon, A. Zafar, M. U. Keerio, W. A. Adil, and A. A. A, "Experimental Study and Analysis of Harmonics Generation in Uncontrolled and Controlled Rectifier Converters," *International Journal of Scientific & Engineering Research*, vol. 5, no. 1, pp. 1343–1350, 2014.

[26] M. A. Hannan, W. Y. Yap, and Y. T. Tan, "Experiment Based Power Quality Learning Issues : A Voltage Sag and Harmonic Case," *Journal of Applied Sciences Research*, vol. 8, no. 10, pp. 4988–4997, 2012.

[27] Fluke Corporation, "Fluke 43B Power Quality Analyzer." [Online]. Available: http://www.fluke.com/fluke/inen/Power-Quality-Tools/Troubleshooting-Power-Meters/Fluke-43B.htm?PID=56080.

[28] S. J. Chapman, "Induction Motors," in *Electric Machinery Fundamentals*, 5th ed., Singapore: McGraw-Hill, 2012, pp. 380–385.

APPENDIX A

Requirement for Class A Performance as Indicated in IEC 61000-4-30

Table 1: Measurement Parameters and Uncertainty Specifications for Main PQ Problem

PQ Problem	Measurement Parameter	Maximum Permissible Error in Class A
Frequency deviation	Power frequency	±0.01 Hz
Fluctuation of the supply voltage	rms value	±0.1% of U_{din}
Light flicker	P_{st} (as in IEC 61000-4-15)	None specified
Voltage dip/ Voltage swell	Residual voltage/ Voltage magnitude	±0.2% of U_{din}
	Duration	1 cycle
Voltage interruption	Duration	2 cycle
Supply voltage unbalance	Negative sequence Zero sequence	±0.15% of positive sequence
Voltage harmonics	Harmonic subgroups	±5% U_m; $U_m \geq 1\%\ U_{din}$ ±0.5% U_{din}; otherwise
Current harmonics	Harmonics subgroups	±5% I_m; $I_m \geq 3\%\ I_{din}$ ±1.5% I_{din}; otherwise
Voltage-current interharmonics	Interharmonics groups	Identical to those given for harmonics subgroups

Table 2: Range of Influence Quantities of the Input Signals for Class A Performance Verification

Influence Quantities	Range of Variation
Frequency	42.5 Hz – 57.5 Hz for 50 Hz systems 51 Hz – 69 Hz for 60 Hz systems
Voltage magnitude (steady-state)	0% - 200% U_{din}
Flicker (P_{st})	0 - 20
Unbalance	0% - 5%
Harmonics (THD)	Twice IEC 61000-2-4, class 3
Interharmonics (at any frequency)	Twice IEC 61000-2-4, class 3
Main signalling voltage	0% - 9% of U_{din}
Transient voltages according to IEC 61180	6 kV peak
Fast transients	4 kV peak

Table 3: Uncertainty Testing States for Class A Performance

Influence Quantities	Testing State 1	Testing State 2	Testing State 3
Frequency	f_{nom} ± 0.5 Hz	f_{nom} – 1 Hz ± 0.5 Hz	f_{nom} + 1 Hz ± 0.5 Hz
Voltage magnitude	U_{din} ±1%	Determined by flicker, unbalance, harmonics, interharmonics (below)	Determined by flicker, unbalance, harmonics, interharmonics (below)
Flicker	P_{st} < 0.1	P_{st} = 1 ± 0.1 – rectangular modulation at 39 changes per minute	P_{st} = 4 ± 0.1 – rectangular modulation at 110 changes per minute NOTE This only applies to 10-min values. For other values, use P_{st} = 0 to 0.1
Unbalance	0% to 5% of U_{din}	0.73% ± 0.5% U_{din} Phase A 0.80% ± 0.5% U_{din} Phase B 0.87% ± 0.5% U_{din} Phase C all phase angle 120°	1.52% ± 0.5% U_{din} Phase A 1.40% ± 0.5% U_{din} Phase B 1.28% ± 0.5% U_{din} Phase C all phase angle 120°
Harmonics	0% to 3% of U_{din}	10% ± 3% of U_{din} 3^{rd} at 0° 5% ± 3% of U_{din} 5^{th} at 0° 5% ± 3% of U_{din} 29^{th} at 0°	10% ± 3% of U_{din} 7^{th} at 0° 5% ± 3% of U_{din} 13^{th} at 0° 5% ± 3% of U_{din} 25^{th} at 0°
Interharmonics	0% to 0.5% of U_{din}	1% ± 0.5% of U_{din} at 7.5 f_{nom}	1% ± 0.5% of U_{din} at 3.5 f_{nom}